

**A
Thesis
On
Studies on Improvement of Surface Characteristics and
Stability of Cr, Cu and Zn Based Metal Organic Frameworks
(MOFs)**

Submitted By

**Gaurav Kumar Chandrakar
(Roll No: 209CH1051)**

**in partial fulfillment of the requirements for the degree in
Master of Technology in Chemical Engineering**

Under the guidance of

Dr. Pradip Chowdhury



**Department of Chemical Engineering
National Institute of Technology Rourkela
May, 2011**

NATIONAL INSTITUTE OF TECHNOLOGY, ROURKELA

DEPARTMENT OF CHEMICAL ENGINEERING



Certificate

Certified that this Project thesis entitled "Studies on Improvement of Surface Characteristics and Stability of Cr, Cu and Zn Based Metal Organic Frameworks (MOFs)" by

Gaurav Kumar Chandrakar

(209 CH 1051)

during the year 2010 - 2011 in partial fulfillment of the requirements for the award of the Degree of Master of Technology in Chemical Engineering at National Institute of Technology, Rourkela has been carried out under my supervision and this work has not been submitted elsewhere for a degree.

Date: 23/05/2011

Guide:

Dr. Pradip Chowdhury
Assistant Professor
Department of Chemical Engineering
National Institute of Technology,
Rourkela

Acknowledgements

First and the foremost, I would like to offer my sincere thanks and gratitude to my thesis supervisor, **Dr. Pradip Chowdhury** for his immense interest and enthusiasm on the project. His technical prowess and vast knowledge on diverse fields left quite an impression on me. He was always accessible and worked for hours with me. Although the journey was beset with complexities but I always found his helping hand when it mattered most. He has been a constant source of encouragement for me.

I am also thankful to all faculties and support staff of Department of Chemical Engineering, Department of Materials and Metallurgical Engineering, Department of Mechanical Engineering and Department of Chemistry, National Institute of Technology, Rourkela, for constant help and extending the departmental facilities for my project work.

I would like to extend my sincere thanks to my friend and colleague, Sankaranarayanan H, for his unconditional assistance and encouragement, for the stimulating discussions, for the sleepless nights we were working together before deadlines, and also to my friends, Vamsi Krishna G and Debalaxmi Pradhan for sincere help extended in completion of my project and for all the fun we have had in the last two years.

Last but not the least, I wish to profoundly acknowledge my parents for their constant support.

Gaurav Kumar Chandrakar
(Roll No: 209 CH 1051)

Dedicated to the memory of

My Grandfather

ABSTRACT

“Metal Organic Frameworks” or MOFs is a term being associated to represent a class of novel adsorbents that has caught the attention of researchers owing to their great diversity in structures resulting from co-ordination bonds between inorganic metal atoms as nodes and organic ligands as linkers. They have high specific surface area (*ca.* 1000-5000 m²/g), large pore volume (*ca.* 0.7-2.5 cc/g) and low to moderate heat of adsorption (*ca.* 12 to 30 kJ/mol at moderate coverage).

Proper selection of metal atoms and organic linkers leads to innumerable possibilities in the coordination geometry with wide variation in topology and functional groups. The tunable matrices or so-called tailor made structures has made it possible to design and synthesize materials meeting specific applications. Porosity, crystallinity and product purity are some of the key features of MOFs. Adsorptive gas separation/purification, gas storage and catalysis are some of the potential areas of study.

Although MOFs have shown tremendous potential, however there remain certain challenges which are typical of this class of adsorbents. Before being explored effectively at the industrial level, it is important to study some of their key features. MOFs are reported to show highest surface area to the tune of *ca.* 1000-5000 m²/g. A careful review of literature has shown a major anomaly though. It is been observed that surface area and pore volume for the same MOF synthesized and reported by different research groups across different laboratories varied considerably. This is even true for different batches of the same MOF synthesized in the same lab. The reasoning behind this can be attributed to various synthesis conditions and post-treatment thereafter. It is been observed that percentages of impurities formed during synthesis

requires a thorough post synthesis treatment to remove all the residual impurities which eventually dictates the “effective surface area” for any gas adsorption study. Thermal and chemical stability of MOFs is another area which needs to be studied carefully. The effectiveness of any MOF adsorbent can be measured from its robustness at high temperature and structural immunity against various organic, inorganic and atmospheric conditions.

We conceived our idea on present research work based on the discussions in the preceding paragraph. Our research objectives can be broadly divided into following sub-sections:

- (I) Synthesizing MOFs of various topologies and tuning the synthesis route for better reproducibility
- (II) Studying thermal and chemical stability of the synthesized materials
- (III) Studying the surface characteristics of the synthesized materials

It is noteworthy to mention here that a careful review of the literature reveals more than 2,000 different MOF structures being synthesized and characterized. Although the number speaks volumes about their variation in structural configuration but the most important in that series include IRMOFs, Cu-BTC and MIL series. For our present research work we have opted for

- (I) Zn-BDC also known as MOF-5 or IRMOF-1
- (II) Cu-BTC more familiarly HKUST-1 or MOF-199
- (III) Cr-BDC popularly known as MIL-101

Synthesis and characterization of Cu-BTC, Cr-BDC and Zn-BDC samples were successfully carried out in our present study. SEM images confirmed the authenticity of each of the MOFs. Cr-BDC and Cu-BTC were found octahedral in shape whereas Zn-BDC crystals appeared to be cubic in nature. The presence of impurities was not uncommon in MOF synthesis and here as

well we had seen reactions leading to the formation of impure by-products. Post synthesis treatments in different organic environments were particularly important in removal of these impurities. Powder XRD patterns validated the crystalline nature of the products formed and thereby degree of purity in various batches owing to different solvent treatments. TGA patterns were typical of specific MOFs synthesized. However, a shift towards low thermal stability had been observed for cases where solvents eliminated impurities. Although it appeared that elimination of impurities decreased the thermal stability of the products but if not, eventually it would lead to reducing the effective surface area which is most crucial in any gas adsorption study. The packing density data nicely corroborated the TGA analysis.

CONTENTS

	PAGE NO.
<i>Abstract</i>	I
<i>List of Tables</i>	VI
<i>List of Figures</i>	VII
CHAPTER 1: Introduction	1
1.1 Prelude	1
1.2 Adsorbents of Importance	5
1.2.1 Zeolites	6
1.3 Research Objectives	9
CHAPTER 2: Literature Review	11
2.1 Metal Organic Frameworks (MOFs)	11
2.1.1 Introduction	11
2.1.2 Potential Research Areas	12
2.2 Description of Framework Structures	14
2.2.1 Cu-BTC or HKUST-1 Framework	14
2.2.2 Cr-BDC or MIL-101 Framework	15
2.2.3 Zn-BDC or MOF-5 Framework	16
2.3 Literature Review on Cu-BTC, Cr-BDC and Zn-BDC MOFs	18

CHAPTER 3:	Experimental Works	21
	3.1 Materials	21
	3.2 Synthesis Procedures	21
	3.2.1 Synthesis of Cu-BTC or HKUST-1	21
	3.2.2 Synthesis of Cr-BDC or MIL-101	22
	3.2.3 Synthesis of Zn-BDC or MOF-5	23
	3.3 Characterization	23
CHAPTER 4:	Results and Discussions	25
	4.1 Surface Morphology of Cr-BDC	25
	4.2 Synthesis of Cr-BDC at Other Reaction Conditions	26
	4.3 Particle Size of Cr-BDC crystals	28
	4.4 The Powder XRD Pattern of Cr-BDC	29
	4.5 Thermogravimetry Analysis of Cr-BDC Samples	30
	4.6 Surface Morphology of Cu-BTC	32
	4.7 The Powder XRD Pattern of Cu-BTC	33
	4.8 Thermogravimetry Analysis of Cu-BTC Samples	35
	4.9 Surface Morphology of Zn-BDC	36
	4.10 The Powder XRD Pattern of Zn-BDC	37
	4.11 Thermogravimetry Analysis of Zn-BDC Samples	39
CHAPTER 5:	Conclusions and Future Scope	40
REFERENCES		41

LIST OF TABLES

Table	Table Caption	Page Number
2.1	Compilation of synthesis and reported surface area of Cu-BTC, Cr-BDC and Zn-BDC MOFs: (I) Cu-BTC (II) Cr-BDC (III) Zn BDC	19
3.1	Summary of Experimental Approaches	22

LIST OF FIGURES

Figure Number	Figure Caption	Page Number
1.1	Schematic diagrams depicting framework structures of two common zeolites, (A) Zeolite A (B) Zeolite X or Y	8
2.1	Schematic for $\text{Cu}_3(\text{BTC})_2(\text{H}_2\text{O})_3$ (BTC= 1,3,5-benzenetricarboxylate) metal organic framework. In this figure Cu-Green, O-Red, C-Gray). For the sake of clarity all hydrogen atoms are not shown	15
2.2	Schematic for Cr-BDC or MIL-101 Framework (a) Inorganic trimer (b) Benzene-1,4-dicarboxylic acid (BDC) (c) Supertetrahedra made from the linkage of inorganic trimers and BDC (d) Schematic view of MIL-101 structure	16
2.3	MOF-5 structure and topology. (a) The MOF-5 structure shown as ZnO_4 tetrahedra (blue polyhedral) (b) The topology of the structure shown as a ball-and-stick model (c) The structure shown as the envelopes of the $(\text{OZn}_4)\text{O}_{12}$ cluster (red truncated tetrahedron) and benzene dicarboxylate (BDC) ion (blue slat)	17
4.1	SEM images of Cr-BDC samples: (A) Impure Cr-BDC (B) DMF washed (C) Cold Ethanol treated (D) Hot Ethanol treated	25
4.2	Cr-BDC synthesized at (A) 180°C and (B) 200°C at high HF concentration	27
4.3	Dimensioning of Cr-BDC crystals (top), average particle size (bottom)	28
4.4	Powder XRD pattern of various batches Cr-BDC samples	29
4.5	TGA pattern of Cr-BDC samples, top (absolute weight loss) & Bottom (% weight loss)	30
4.6	SEM images of Cu-BTC samples	32
4.7	Powder XRD pattern of various batches Cu-BTC samples	33
4.8	TGA pattern of Cu-BDC samples	35
4.9	SEM images of Cu-BTC samples	36
4.10	Powder XRD pattern of various batches Zn-BDC samples	38
4.11	TGA pattern of Zn-BDC samples	39

CHAPTER 1

INTRODUCTION

1.1 Prelude

The concept of adsorption was conceived as early as eighteenth century by Scheele and Fontana when they observed porous solids to reversibly adsorb vapors but the practical applications of this property largely remain unexplored. A few familiar practical examples that were practiced in earlier times include removal of moisture from gas streams using suitable hydrophilic agents in driers, removal of impurities such as H_2S and mercaptans from natural gas, removal of harmful organic pollutants from water etc. [1, 2]. The above processes are very much still in vogue and are classified as purification processes. Major advances in the field of adsorption took place in the latter half of the twentieth century with the advent of new adsorbents mainly *zeolites* and development of efficient process cycles.

Although first synthetic zeolite was synthesized by Milton at the Union Carbide Corporation but the history of this class of adsorbent goes dates back. It all started with the discovery of a mineral called “*stilbite*” by a Swedish mineralogist Crönsted. The said mineral showed intumescence when heated in a flame and this new family of material was named “*zeolite*”. The etymology of the word “zeolite” explains its origin from Greek words “zeo” and “lithos” meaning “to boil” and “stone”. Since then for most of the times natural zeolite crystals were making their presence felt in “museums” to the amusement of the visitors till the advent of first man-made synthetic

zeolites [3]. Simultaneously new and efficient process cycles were developed and adsorption established itself as one of the major unit operations in process industries.

All adsorption separation processes involve two principal steps. They are: (a) *adsorption*, when one component is being preferentially adsorbed onto the solid from its mixture and (b) *desorption* or *regeneration*, during which the adsorbent bed is cleaned to be used for the next cycle. Adsorptive separation processes can be categorized on certain principles. They are summarized as [1]:

- (I) *Based on mechanism of separation:* Adsorptive separation is achieved by one of the following three mechanisms: steric, kinetic and equilibrium. Steric effect is also known as size-selective sieving. Here the microporous adsorbent allows only the smaller molecule (diameter of the molecule is comparable with the dimension of the micropore) to pass through whereas larger size molecules are totally excluded. Adsorbents e.g. zeolites having uniform pore size distribution shows steric effect. A common example is separation of linear from branched and cyclic hydrocarbons on 5A zeolite. Kinetic separation is achieved due to the differences in diffusion rates of different molecules. It is achieved with adsorbents of varying pore size distribution. A classic example is the separation of N_2 from Air using molecular sieve carbon. Equilibrium separation on the other hand depends on the differences between relative affinities of the adsorbent towards various adsorbates. Majority of the adsorption processes operate through equilibrium mechanism.
- (II) *Based on feed composition:* The separation processes may also be divided in the line of feed concentration. Based on feed concentration the separation process may be

divided into bulk separation and purification. As had been defined by Keller [1], bulk separation is the point when 10 wt% or more of the mixture is adsorbed. Purification processes are generally separation processes when the components adsorbed are generally present in low concentration, have little economic value and are not recovered.

- (III) *Based on method of adsorbent regeneration:* Adsorbents can be regenerated by several mechanisms. Widely used ones include temperature swing adsorption (TSA) cycles, pressure swing adsorption (PSA) cycles, purge gas stripping and displacement desorption. TSA cycles are run on heating-cooling mechanism whereas PSA process involves steps like: pressurization-adsorption-countercurrent blowdown and countercurrent purge. PSA processes are fast whereas each heating-cooling cycle in a TSA process requires a lot of time and used exclusively for processes, in which the amount of adsorptive gases being processed are small. Apart from TSA and PSA, other regeneration processes include purge gas stripping and displacement desorption. In inert purge gas stripping cycle, the adsorbent is regenerated by passing a non-adsorbing and weakly adsorbing gas through the adsorber without changing the temperature or pressure. The void in the bed is filled with the inert gas upon completion of regeneration. However, in a displacement desorption a gas or vapor that adsorbs about as strongly as the adsorbate is used; regeneration is thus facilitated both by adsorbate partial-pressure reduction and by competitive adsorption of the displacement medium [1]. Displacement desorption process requires more complex scheme of operation and is used only in situations where rest of the processes fail. Some important examples of displacement desorption technique are MOLEX and

PAREX processes. The MOLEX process uses the Sorbex simulated moving bed technique (developed by UOP) to recover high purity n-paraffins by continuous adsorptive separation. This technique is similar in concept to liquid chromatography, but carried out on a large commercial scale. UOP's PAREX process is used for the recovery of *para*-xylene from mixed xylenes that offers high product purity, high product recovery, high efficiency and extended adsorbent life. "Mixed xylenes" is a mixture of C₈ aromatic isomers that includes ethyl benzene, *para*-xylene, *meta*-xylene, and *ortho*-xylene. They boil so closely together that separation by distillation is not practical. PAREX process provides an efficient means of recovering *para*-xylene using a zeolitic adsorbent [1-2]

The importance of adsorption based processes can be gauged from situations when other conventional separation processes don't perform efficiently. A few typical cases are given below [1]:

- (I) Although process simplicity and scalability is the reason behind popularity of distillation over other unit operations, however when the relative volatility between the key components to be separated is less than 1.2 to 1.5 or even lesser, distillation becomes highly energy intensive and fails when relative volatility is unity. In such cases, alternate separation mechanisms like adsorption yield better result. Adsorption based separation techniques can be highly efficient because of high separation factors achievable between the key components by pragmatic selection of a suitable zeolite. Separation of isomers e.g. n-paraffin from iso-paraffin using 5A molecular sieve, separation of iso-paraffins, iso-olefins from di-n-butylamine using 10X molecular

sieve are the examples where adsorptive separation are more effective than distillation [1, 2].

- (II) When the component of our interest is present in low concentration and bulk of the feed is of low-value, adsorption is preferred to distillation.
- (III) When the two groups of components to be separated are having overlapping boiling ranges, adsorption based separation is effective if they contain chemically or geometrically dissimilar molecules.

1.2 Adsorbents of Importance

The success and failure of any adsorption based system largely depends on the selection of a proper adsorbent for a particular application. Although literature is crowded with examples of various adsorbents but only a few could last over the ages of technological advances. Some well known adsorbents are: silica gel, activated alumina, activated carbon, carbon molecular sieves and zeolites. Each of these adsorbents has certain specific features that have been exploited in various applications ranging from adsorptive separation/purification, ion-exchange and catalysis.

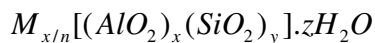
The primary classification between the adsorbents shows two distinct types of surfaces: 'hydrophilic' and 'hydrophobic'. Such type of behavior can be attributed to the surface polarity (as a result of presence of ions in the structure) of the adsorbents. Polar adsorbents *viz.* zeolites, activated alumina, silica gel etc. show a tremendous affinity towards polar molecules whereas non-polar activated carbon shows little or no affinity towards polar adsorbates. Zeolites owe their hydrophilic nature to the polarity of the heterogeneous surface whereas presence of hydroxyl groups on the surface of silica gel or activated alumina is largely responsible for their

‘hydrophilicity’ by hydrogen bond formation. These features are particularly important for consideration during equilibrium based separation processes. The fundamental physical properties of the targeted adsorbate molecule like polarizability, permanent dipole moment, quadrupole moment, magnetic susceptibility in comparison with the other molecules present in the mixture needs to be examined in detail at first before sorbent design or selection.

The most important feature of any adsorbent material is their porosity. Basically, a highly porous material possess high specific surface area and total pore volume. Pore size distribution is also an important consideration during physical characterization of a porous material. Parameters like bulk density, crush strength and erosion resistance are also important considerations while characterizing any solid adsorbent before practical applications. International Union of Pure and Applied Chemistry (IUPAC) categorized porous materials into three different categories by size: microporous (<2 nm), mesoporous (2-50 nm) and macroporous (>50 nm). Within the microporous regime, there exists a fundamental difference between different adsorbents. For adsorbents like silica gel, activated carbon or activated alumina there is a distribution of micropore size whereas in a zeolitic adsorbent since the micropore size is controlled by the crystal structure there is virtually no distribution of pore size. This unique feature of zeolites leads to significant results in adsorption properties and set them apart from other conventional adsorbents.

1.2.1 Zeolites

Zeolites are crystalline aluminosilicates of alkali or alkali earth elements, such as sodium, potassium and calcium. The chemical composition of zeolites can be represented by the following stoichiometry:



Where x and y are integers with y/x equal to or greater than 1, n is the valance of cation M , and z is the number of water molecules in each unit cell [1]. The zeolite framework basically consists of an assemblage of SiO_4 and AlO_4 terahedra, joined together in various regular arrangements through shared oxygen atoms, to form an open crystal lattice containing pores of molecular dimensions. Since the crystal lattice determines the micropore structure, it results into pores of uniform size with no distribution, a feature very unique amongst adsorbents.

In the zeolite framework each aluminium atom introduces one net negative charge and must be balanced by an exchangeable cation. Replacing the cation by means of ion exchange imparts exciting adsorptive properties into the structure and had been widely exploited. The water molecules present within the framework can be removed easily by simple heating or evacuation which leaves almost an unaltered skeleton with a void fraction varying between 0.2-0.5. The Si/Al ratio is very important in a zeolite framework. Generally the ratio is never less than one but there is no upper limit to it. The adsorption properties show a systematic shift as ratio changes from Aluminium rich to Silicon rich. Aluminium rich zeolitic frameworks are hydrophilic and have very high affinities for water and other polar molecules whereas microporous silicas (Si rich) *viz.* silicalite are hydrophobic. The transition from hydrophilic to hydrophobic character generally occurs at a Si/Al ratio ranging from 8 to 10. Thus the adsorptive properties of zeolites vary considerably with Si/Al ratio and cationic form of the framework [1, 2].

There are different types of zeolitic frameworks cited in literature [2]. A few examples are given below:

(A) Sodalite (the channels are constricted by six-membered oxygen rings with free diameter of about 2.8 Å).

(B) “Small-pore” zeolites such as Type A, Chabazite, and Erionite (access is through eight-membered oxygen rings with free diameter of 3.0-4.5 Å).

(C) “Medium-pore” pentasil zeolites include names such as ZSM-5, ZSM-11, and Silicalite (characterized by ten-membered oxygen rings and intermediate channel with free diameter of 4.5-6.0 Å).

(D) “Large-pore” zeolites such as Type X, Type Y, and Mordenite (access is through twelve-membered oxygen rings with free diameter of 7.0-7.4 Å).

The schematic representation of two zeolite framework structures is given below:

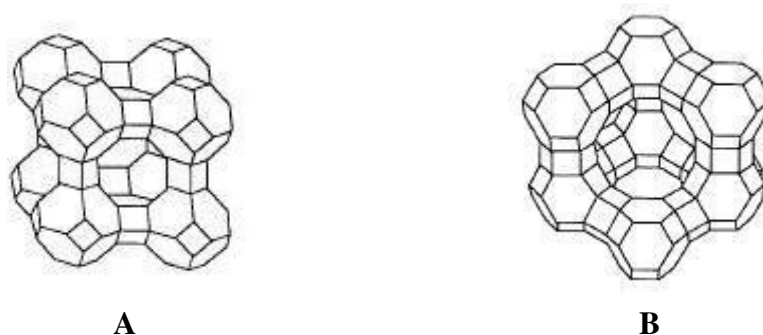


Figure 1.1: Schematic diagrams depicting framework structures of two common zeolites, (A) Zeolite A (B) Zeolite X or Y [1, 2].

The structural unit in both Type A zeolite and Types X and Y, is the truncated octahedron as shown in Fig. 1.1. The unit is also known as sodalite cage or beta cage. The four member rings

of the sodalite units are linked through four member prisms, which assemble into Type A framework. The free diameter in the central cavity is 11.4 Å, which is entered through six eight member oxygen-ring apertures with a minimum diameter of 4.4 Å. In case of Type X and Y zeolite frameworks the sodalite units are linked through six member prisms and the aperture is formed by the 12 member oxygen rings with a free diameter of approximately 7.4 Å.

Although ‘Zeolite’ was discovered in the eighteenth century, it took approximately another century before practical applications of this class of material was realized e.g. reversible adsorption-desorption of water, ion-exchange etc. By the advent of the 20th century its potential in various other fields materialized e.g. adsorption of organic and smaller molecules etc. Soon the shape-selective nature was noted and in 1932, McBain coined the term ‘molecular sieve’ to the zeolite minerals [4].

1.3 Research Objectives

Our research objectives can be broadly classified into following sub-sections:

- (A) Synthesizing MOFs of various topologies and tuning the synthesis route for better reproducibility
- (B) Studying thermal and chemical stability of the synthesized materials
- (C) Studying the surface characteristics of the synthesized materials

It is noteworthy to mention here that a careful review of literature reveals more than 2,000 different MOF structures being synthesized and characterized. Although the number speaks volumes about MOFs’ variation in structural configuration but the most important in that series include IRMOFs, Cu-BTC and MIL series. For our present research work we have opted for

- (I) Zn-BDC also known as MOF-5 or IRMOF-1
- (II) Cu-BTC more familiarly HKUST-1 or MOF-199
- (III) Cr-BDC popularly known as MIL-101

2.1 Metal Organic Frameworks (MOFs)

2.1.1 Introduction

“Metal Organic Frameworks” or MOFs represent a class of novel materials that has caught the attention of researchers owing to their great diversity in structures resulting from co-ordination between inorganic metal atoms/ions and organic ligands as linkers. Proper selection of metal atoms/ions and organic linkers leads to innumerable possibilities in the co-ordination geometry with wide variation in structural architecture. A few very attractive motifs include honeycomb, brickwall, bilayer, ladder, herringbone, diamondoid, rectangular grid, and octahedral geometries [5-12]. The inorganic part in a MOF topology invariably (with a few exceptions) consists of first-row transition metals whereas organic links such as cyanide, glutamate, formate, triazole, oxalate, carboxylate, and squarates are well known [5, 7-19]. MOFs are crystalline porous solids composed of a 3-D network of metal ions held in place by multidentate organic molecules where the spatial organization of these structural units results to a system of channel and cavities in the nanometer length scale. The ‘tunable matrices’ or so-called ‘tailor made’ structures of MOFs has made it possible to design and synthesize materials meeting specific applications.

Although references cited in some review articles highlighted the concept of novel solids was introduced as early as sixties however history of these materials goes dates back (early examples are Hofmann type clathrates, Prussian-Blue type structures, and Werner complexes) but the true interest in this field of synthesizing MOFs generated decades later [20-21]. MOF-5 was reported

[22] and published in 1999. The inability of these solids to maintain permanent porosity and avoid structural rearrangements upon guest removal or guest exchange, leading to complete collapse of the framework has an obvious shortcoming initially. MOFs exhibiting permanent porosity have been reported later.

2.1.2 Potential Research Areas

Ever since the first successful synthesis of a metal organic framework (MOF-5) there has been a continuous surge in research activities in this field. The concept of reticular design enables ‘tailoring’ a MOF structure with regular porosity at the nanometer scale. ‘Tunability’ coupled with very high ‘surface area’ and ‘pore volume’ made metal organic frameworks a very interesting proposition for research in various fields. MOFs are highly crystalline with very low crystalline framework densities and interestingly most of the pores fall under IUPAC microporous regime i.e. < 2 nm and can be synthesized in very pure form. The salient features and beneficial traits shown by MOFs attracted researchers across the globe to exploit its potentials.

Buoyed by the success of MOF-5, a major focus of the researchers turned onto synthesizing novel materials or frameworks that involves a simple and pragmatic choice of metal atoms and organic linkers as building blocks. Their intriguing features raised enough speculations in different quarters and till date more than 2,000 MOF structures with compositional and architectural diversity have been synthesized, unparalleled by any other class of materials. The most widely studied MOF series since its inception can be grouped as follows:

- (I) The Isorecticular Metal Organic Framework or IRMOF series (MOF-5 being also known as IRMOF-1).

- (II) Cu-BTC or HKUST-1.
- (III) Matériel Institut Lavoisier or MIL series

Although the number speaks volumes about their variation in structural configuration but not all them are stable. Thermal and chemical stability, along with high surface area is what researchers look for in a good material to be effective at the industrial level. Structural aspects of these adsorbents mainly improved synthesis procedures and better activation methods along with gas adsorption studies primarily focusing on H₂ storage had been carried out and cited in different articles. Interesting results on CO₂ and CH₄ adsorptions were reported in various articles. Molecular simulations explaining “host-guest” interactions were explained in detail by various research groups. A thorough review of various research articles identifies the following areas where major research activities are going on:

- (I) Adsorptive separation/purification [23-27]
- (II) Gas storage [28-32]
- (III) Heterogeneous catalysis [33-37]

Apart from these aspects, the potential of MOF materials are also being investigated in areas like non-linear optics, microelectronics and healthcare [38-42].

2.2 Description of Framework Structures

In the following paragraphs we have illustrated the framework architecture of Cu-BTC, Cr-BDC and Zn-BDC metal organic frameworks.

2.2.1 Cu-BTC or HKUST-1 Framework

Cu-BTC [$\text{Cu}_3(\text{BTC})_2$, BTC = 1,3,5-benzenetricarboxylate] also known as HKUST-1 is a widely studied MOF. It was first reported by Chui et al. [44] in 1999. In this framework, two octahedrally co-ordinated Cu atoms are connected to eight oxygen atoms of tetracarboxylate units to form a dimeric Cu paddle wheel. Each BTC ligand holds three dimeric Cu paddle wheels to form a microporous open framework with face-centered cubic symmetry.

Cu-BTC has a 3-D channel structure connecting a system of tetrahedral-shaped cages accessible through small windows (ca. 3.5 Å in diameter). The large cavities are connected through square-shaped windows with a diameter of ca. 9 Å. Fig. 2.1 shows the structure schematically.

The importance of Cu-BTC can be gauged from the fact that ever since Chui and his colleagues reported this co-ordination polymer, there was a growing interest generated in the following years leading to the improvisation of the synthesis methods and better activation procedures resulting into more stable and highly porous solids. Research in various areas *viz.* gas separation, storage and catalysis has been going on presently. It won't be an exaggeration to mention that Cu-BTC turns out to be one of the most sought after adsorbent at the research level.

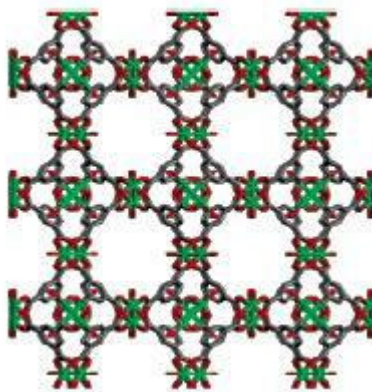


Figure 2.1: Schematic for $\text{Cu}_3(\text{BTC})_2(\text{H}_2\text{O})_3$ (BTC= 1,3,5-benzenetricarboxylate) metal organic framework. In this figure Cu-Green, O-Red, C-Gray). For the sake of clarity all hydrogen atoms are not shown [44, 45].

2.2.2 Cr-BDC or MIL-101 Framework

Cr-BDC [BDC = 1,4-benzenedicarboxylate] framework or MIL-101 (an acronym for Matériau Institut Lavoisier) is a recent addition to the ever increasing list of metal organic frameworks. Férey et al. [46] first synthesized and reported this chromium-terephthalate based solid. The synthesized product showed a very high specific surface area and pore volume. They reported MIL-101 to be very stable for months under ambient atmosphere. The structure remains stable at high temperature (up to 473 K) and in presence of different organic solvents. These properties make MIL-101 an attractive candidate for adsorption study of various gases.

MIL-101, the hybrid solid is synthesized from carboxylate moieties (benzene-1,4-dicarboxylate or bdc) and trimeric chromium(III) octahedral clusters having removable terminal water molecules and therefore provide potential unsaturated metal sites in the structure. The resulting zeotype architecture as shown in Fig. 2.2 are built by the connection of large hybrid supertetrahedra which further assemble to form very large mesopores. The cell volume for MIL-

101 is ca. 702, 000 Å³. Removal of guests results into an accessible diameter of size ~29 Å and 34 Å.

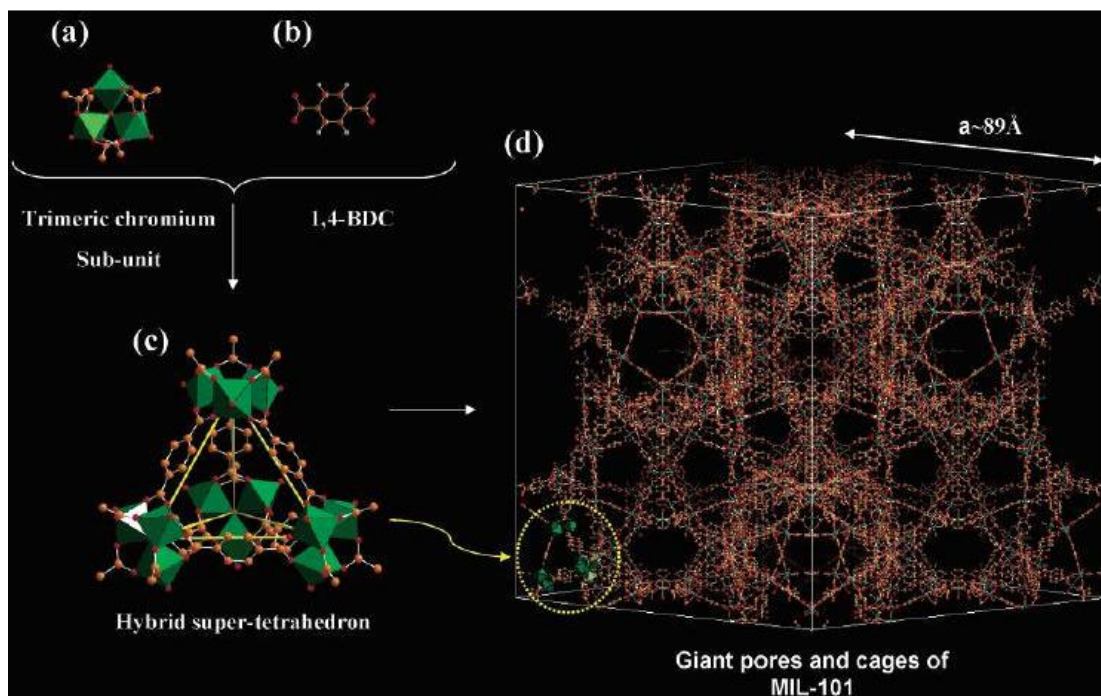


Figure 2.2: Schematic for Cr-BDC or MIL-101 Framework (a) Inorganic trimer (b) Benzene-1,4-dicarboxylic acid (bdc) (c) Supertetrahedra made from the linkage of inorganic trimers and bdc (d) Schematic view of MIL-101 structure [46-47].

2.2.3 Zn-BDC or MOF-5 Framework

MOF-5 consists of Zn^{2+} and 1,4-benzenetricarboxylate. Fig. 2.3 shows the structure and topology of MOF-5.

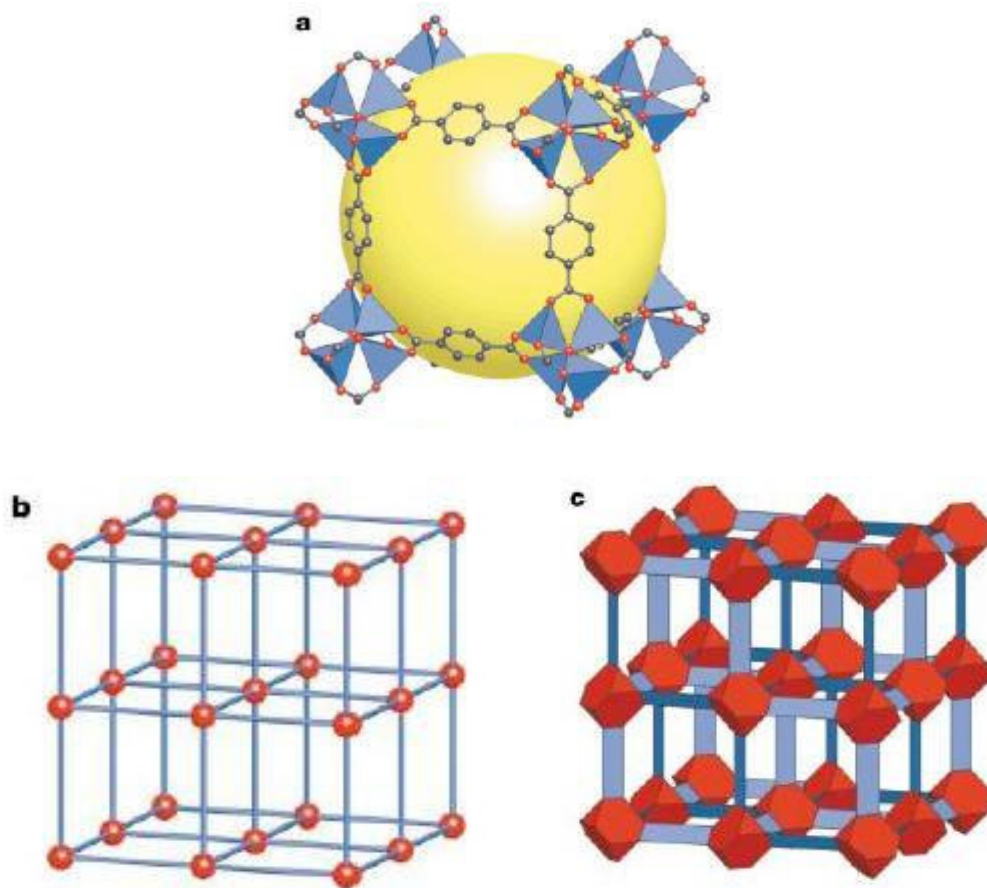


Figure 2.3: MOF-5 structure and topology. (a) The MOF-5 structure shown as ZnO_4 tetrahedra (blue polyhedral) (b) The topology of the structure shown as a ball-and-stick model (c) The structure shown as the envelopes of the $(\text{OZn}_4)\text{O}_{12}$ cluster (red truncated tetrahedron) and benzene dicarboxylate (BDC) ion (blue slat) [5].

In MOF-5, $\text{Zn}_4\text{O}(\text{CO}_2)_6$ units containing four ZnO_4 tetrahedra with a common vertex and six carboxylate carbon atoms that define an octahedral secondary building unit (SBU) are joined together by benzene links. This leads to a cubic network in which the vertices are the octahedral SBUs and the edges are the benzene struts. In practice, this compound was prepared from $\text{Zn}(\text{II})$ and BDC acid under pre-determined conditions to effect the octahedral SBU in situ. Since the SBU and the benzene links are relatively large and rigid entities, the structure produced has exceptional porosity and large micropore volume (larger than any known zeolite). The stability

of the said framework is also very high. The exceptional stability of MOF-5 can be understood by comparing its basic network, composed of single atom vertices (Fig. 2.3(b)) with the actual structure of MOF-5 (Fig. 2.3(a)) which has cationic clusters at the vertices. The basic network has no resistance to shear if the links are considered to be universal joints. However, in actual MOF-5 structure, the cationic cluster has a truncated tetrahedral envelop (Fig. 2.3(c)), and the rigidly planar $\text{O}_2\text{C}-\text{C}_6\text{H}_4-\text{CO}_2$ linkers have a planar slat envelop. The linkage of these two groups produces an inherently rigid structure held together by mutually perpendicular hinges.

2.3 Literature Review on Cu-BTC, Cr-BDC and Zn-BDC MOFs

A comprehensive table has been prepared after going through literature on these said MOFs. The emphasis was put on the various synthesis procedures adopted by research groups and the final surface area and pore volume of the prepared samples. The complete list is given below.

Table 2.1: Compilation of synthesis and reported surface area of Cu-BTC, Cr-BDC and Zn-BDC

MOFs: (I) Cu-BTC (II) Cr-BDC (III) Zn-BDC

(I)

Sl. No	MOF	Synthesis Method	Surface Area (m ² /g)	Pore Volume (cm ³ /g)	References
1	Cu-BTC	Hydrothermal	1482	0.828	[48]
2		Hydrothermal	698	0.39	
3		—	1635	0.82	
4		—	1504	—	
5		Hydrothermal	692	0.333	[44]
6		Hydrothermal	964,1333 (different batch)	0.658	[49]
7		Hydrothermal	—	0.37	[50]
8		Hydrothermal	—	0.41	[34]
10		Electrochemical	—	—	[51]
11		Hydrothermal	1781	—	[52]
12		Hydrothermal	1507	0.75	[53]
18		Hydrothermal	—	0.32	[54]

(II)

Sl. No	MOF	Synthesis Method	Surface Area (m ² /g)	Pore Volume (m ³ /g)	References
1	MIL-101	Hydrothermal	3197	1.73	[55]
2		Hydrothermal	3148	1.53	
3		Hydrothermal	2250	1.24	
4		Hydrothermal	2800	1.37	[56]
5		Hydrothermal	3780	1.74	
6		Hydrothermal	4230	2.15	
7		Hydrothermal	2931	1.45	[57]
8		Hydrothermal	2220	1.13	[31]

(III)

Sl.No	MOF	Synthesis Method	BET (m ² /g)	Pore Volume (cm ³ /g)	References
1	Zn-BDC	Solvothermal	–	0.61-0.54	[58]
2		Solvothermal	666	0.21	[59]
3		Solvothermal	650	0.2	
4		Solvothermal	3362	–	[60]
5		Solvothermal	572	0.28	[61]
6		Solvothermal	2296	–	[62]

CHAPTER 3

EXPERIMENTAL WORKS

This chapter revolves around discussing various synthesis procedures on MOFs of our interest (hydrothermal/ solvothermal) and their detailed characterization.

3.1 Materials

All materials were used as supplied by the vendors without further purification. The list of all the chemicals with their formula and manufacturer are shown in the respective parenthesis:

Chromium (III) nitrate Nonahydrate [$\text{Cr}(\text{NO}_3)_3 \cdot 9\text{H}_2\text{O}$, Loba Chemie], Copper (II) Nitrate Trihydrate [$\text{Cu}(\text{NO}_3)_2 \cdot 3\text{H}_2\text{O}$ (Merck)], Zinc (II) Nitrate Hexahydrate $\text{Zn}(\text{NO}_3)_2 \cdot 6\text{H}_2\text{O}$ [Merck], 1,4-benzene dicarboxylic acid [$\text{C}_8\text{H}_6\text{O}_4$, Loba Chemie], Hydrofluoric acid [HF, Merck], 1, 3, 5-benzene tricarboxylic acid (commonly known as trimesic acid) [Merck], N, N-dimethylformamide [Merck], Ethanol [Merck] and Methanol [Merck].

3.2 Synthesis Procedures

3.2.1 Synthesis of Cu-BTC or HKUST-1

Cu-BTC or HKUST-1 was first reported by Chui et al. [44]. This present method was reported by Liu et al. [48] and was a modification of previous works by Rowsell and Yaghi [53]. 1, 3, 5-benzenetricarboxylic acid (1.0 g) was dissolved in 30 ml of a 1:1 mixture of ethanol/*N*, *N*-dimethylformamide (DMF). In another flask, Copper (II) Nitrate trihydrate (2.077 g) was dissolved in 15 ml water. The two solutions were then mixed and stirred for 10 min. They were

then transferred into Teflon-lined stainless steel autoclave and heated at 373 K for 10 hours. The reaction vessel was cooled to room temperature normally. The resulting blue crystals were isolated by filtration and extracted with methanol overnight using a Soxhlet extractor to remove solvated DMF. The product was then dried at room temperature.

3.2.2 Synthesis of Cr-BDC or MIL-101

In a typical synthesis procedure, Cr-BDC or MIL-101 was synthesized hydrothermally following the published work of Férey et al. [46]. The reaction was carried out in a Teflon lined stainless steel autoclave where a stoichiometric mixture of $\text{Cr}(\text{NO}_3)_3 \cdot 9\text{H}_2\text{O}$ (1 gm), de-ionized water (12 ml), 1,4-benzenedicarboxylic acid (0.4 gm) and HF (0.125 ml) was placed for 8 hrs at 493 K. An attempt was made to establish the effect of HF in Cr-BDC synthesis by varying temperature and HF concentration, presented in form of table shown below.

Table 3.1: Summary of Experimental Approaches

Exp Run No	Chromium Nitrate (gm)	Water (ml)	BDC (gm)	HF (ml)	Temperature (°C)	Remarks
1	1	12	0.4	0.125	220	As reported by Férey et al. [46]
2	1	12	0.4	1	120	High HF at lower temperature
3	1	12	0.4	1	180	High HF at high temperature
4	1	12	0.4	0.25	220	High HF at high temperature

Post-synthesis treatments of MIL-101 sample were crucial since significant amount of needle shaped colorless crystals of terephthalic acid (H_2BDC) formed as a by-product. Post treatment synthesis included washing with DMF, Normal Ethanol and Hot Ethanol (70°C) in which sample are treated with solvents under agitation for 5 hours to remove maximum impurity from porous matrix.

3.2.3 Synthesis of Zn-BDC or MOF-5

Zn-BDC was synthesized following the original procedure described by Henrik Fanø Clausen et al. [63] followed by the modified route of Jinping Li et al. [64]. $\text{Zn}(\text{NO}_3)_2 \cdot 6\text{H}_2\text{O}$ (6 g), and H_2BDC (1.7 g) were dissolved in DMF (20 ml). The solution was then transferred into Teflon-lined autoclave, which was heated at 373 K for 24 h. The reaction products were cooled to room temperature, and the solid obtained were collected by centrifugation, washed with DMF, and dried at room temperature.

3.3 Characterization

Thermal analysis of Cu-BTC, Cr-BDC and Zn-BDC samples were carried out in detail in a TGA apparatus, SHIMADZU (DTG 60 H). The morphologies of the synthesized Cu-BTC, Cr-BDC and Zn-BDC products were characterized using a scanning electron microscope (SEM, JEOL JSM-6480 LV) equipped with an energy dispersive X-ray spectrometer (EDX). The different batches of synthesized MOF samples were analyzed by comparing images taken in an optical microscope (Hund Wetzlar H600). The synthesized samples were subjected to X-ray diffraction by a diffractometer (XRD, Philips Analytical, PW-3040) equipped with the graphite monochromatized $\text{CuK}\alpha$ radiation ($\lambda=1.5406\text{\AA}$) in 2θ angles ranging from 5° to 75° with a step size of 0.05 degree and scanning rate 1 minute. The packing density of all batches of MOF

samples were measured by packing an activated sample in a known volume. The sample was then weighed for calculating the density.

4.1 Surface Morphology of Cr-BDC

The scanning electron microscopy images of various batches of Cr-BDC metal organic framework is shown in the following figure.

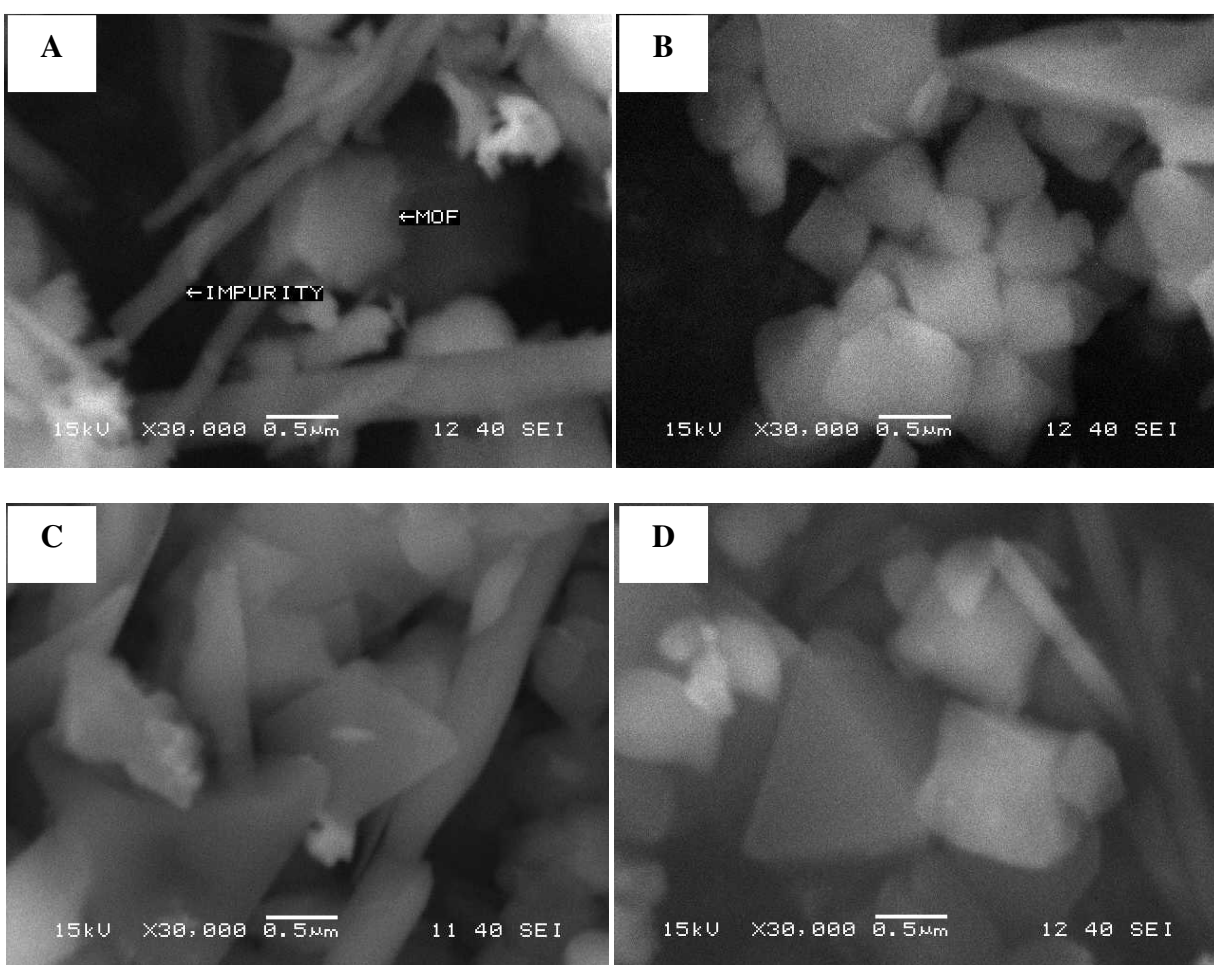


Figure 4.1: SEM images of Cr-BDC samples: (A) Impure Cr-BDC (B) DMF washed (C) Cold Ethanol treated (D) Hot Ethanol treated

It is amply clear from the images that as-synthesized or impure batch of Cr-BDC is contaminated with cylindrical shaped crystals. A thorough study of the reaction chemistry and literature review reveals the fact that during synthesis of Cr-BDC, a large quantity of benzene dicarboxylic acid (or, H₂BDC) forms as the reaction by-product. A DMF wash apparently removes bulk of these BDC crystals (Fig. 4.1(B)). A thorough wash with cold ethanol was tried on the same batch of Cr-BDC. Although ethanol removes BDC crystals but the effectiveness is not as good as DMF (Fig. 4.1(C)).

4.2 Synthesis of Cr-BDC at Other Reaction Conditions

The ideal condition for synthesis of Cr-BDC is at 220°C for 8 hours. We tried to bring down the reaction temperature to 200°C or less with the aim to get a better product (since high temperature tend to produce by-products) and to prolong the longevity of the Teflon lining of the high pressure autoclave. The various permutations and combinations with the temperature, time and reactant concentrations are already shown in table 3.1.

The SEM images of some of the batches are shown in the following figure.

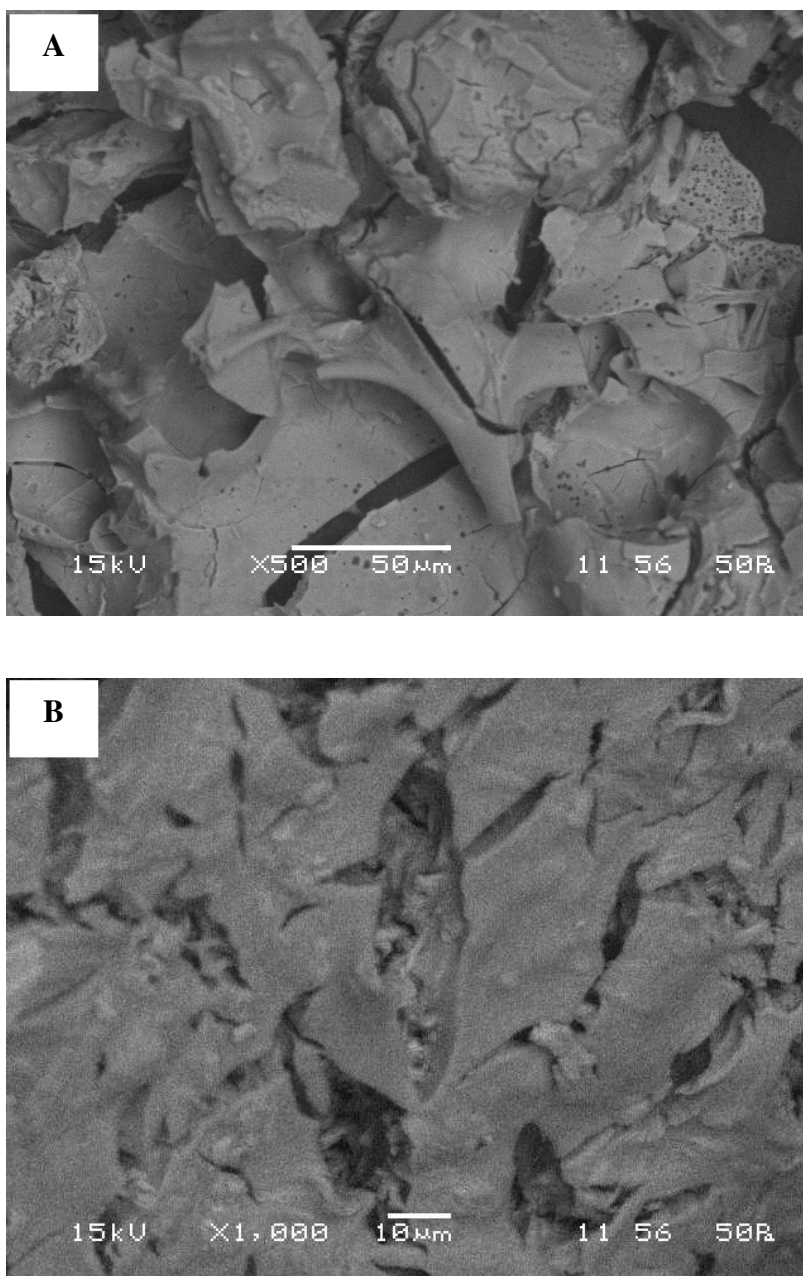


Figure 4.2: Cr-BDC synthesized at (A) 180°C and (B) 200°C at high HF concentration

It is clear from the images that low temperature synthesis doesn't yield any product. Additionally, presence of high concentration of HF tends to fuse the crystals and hence no effective octahedral shaped crystals result.

4.3 Particle Size of Cr-BDC crystals

Although particle size of crystals can be readily measured with laser particle size analyzer, but for our study “*Digimiser*” software was used to calculate the particle size of Cr-BDC crystals.

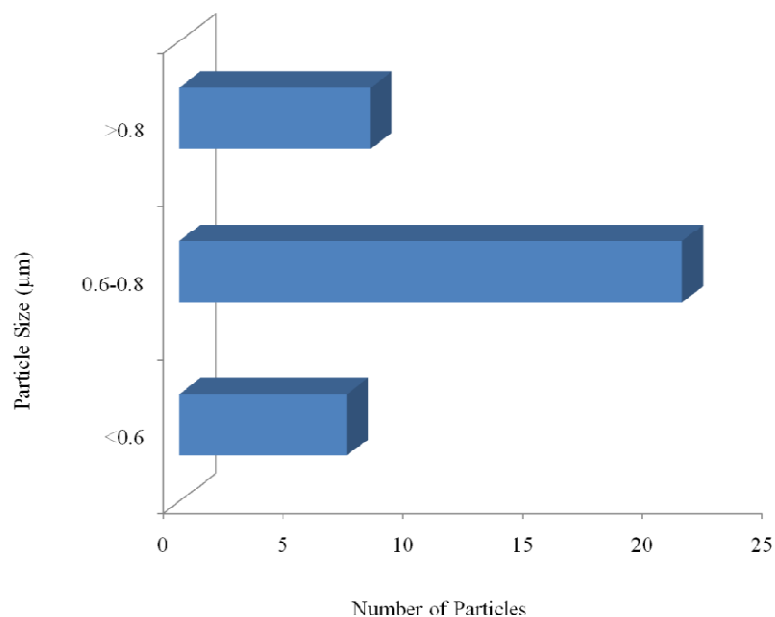
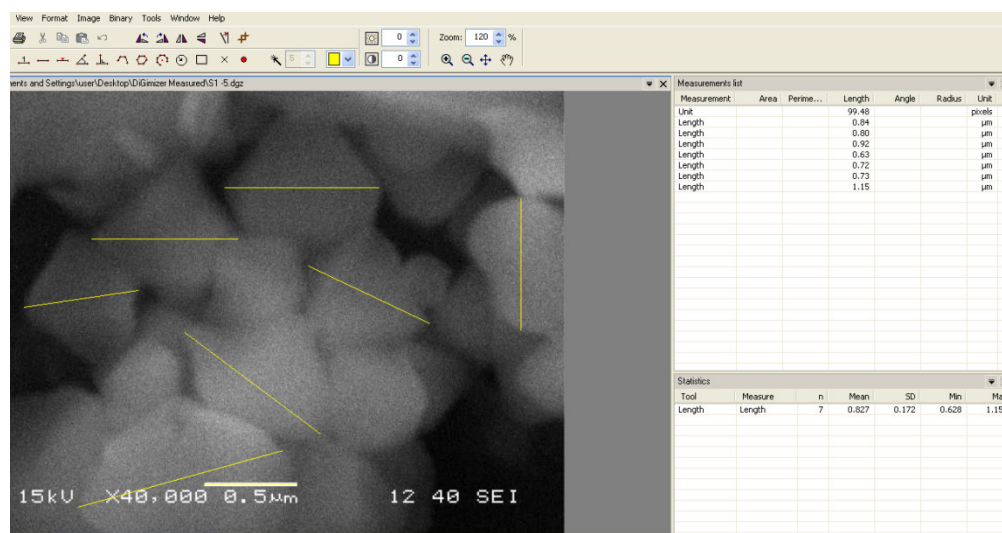


Figure 4.3: Dimensioning of Cr-BDC crystals (top), average particle size (bottom)

The image and the ensuing graph categorically show the average particle size of Cr-BDC particles to be *ca.* 0.6 to 0.8 μm .

4.4 The Powder XRD Pattern of Cr-BDC

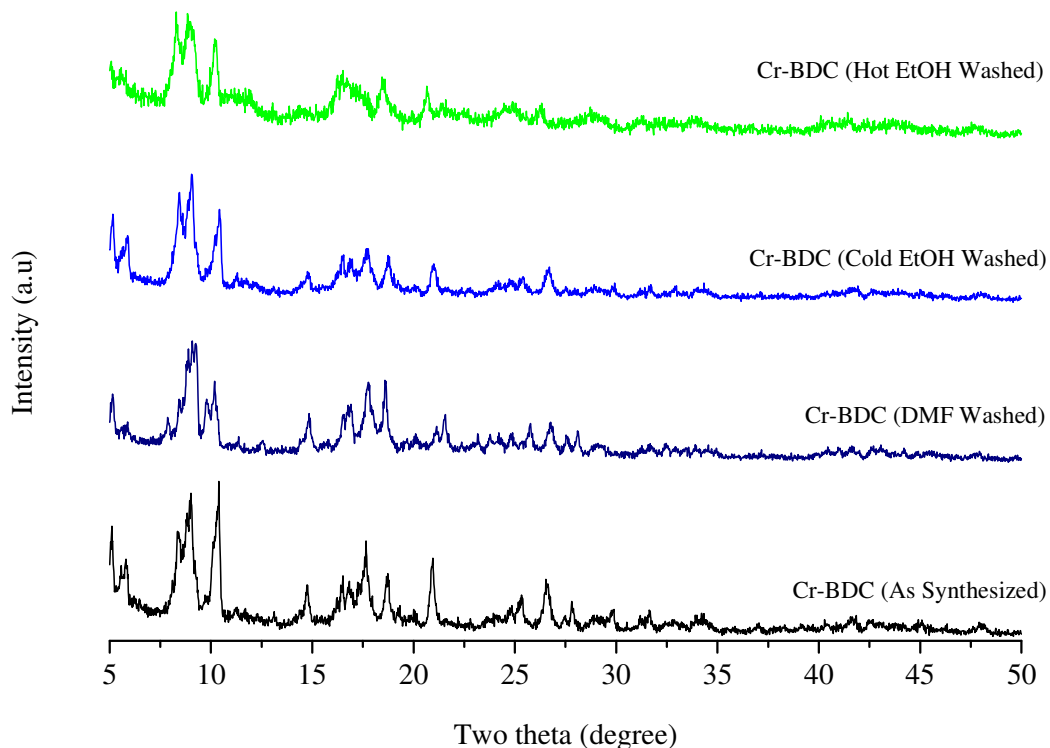


Figure 4.4: Powder XRD pattern of various batches Cr-BDC samples

The XRD pattern clearly shows the crystalline nature of the products formed. The purity of the products improved with every wash as is clearly visible from the diminishing peaks in the higher 2-theta range. As the surface gets rid of H_2BDC impurities, major peaks concentrated in the lower range of 2-theta.

4.5 Thermogravimetry Analysis of Cr-BDC Samples

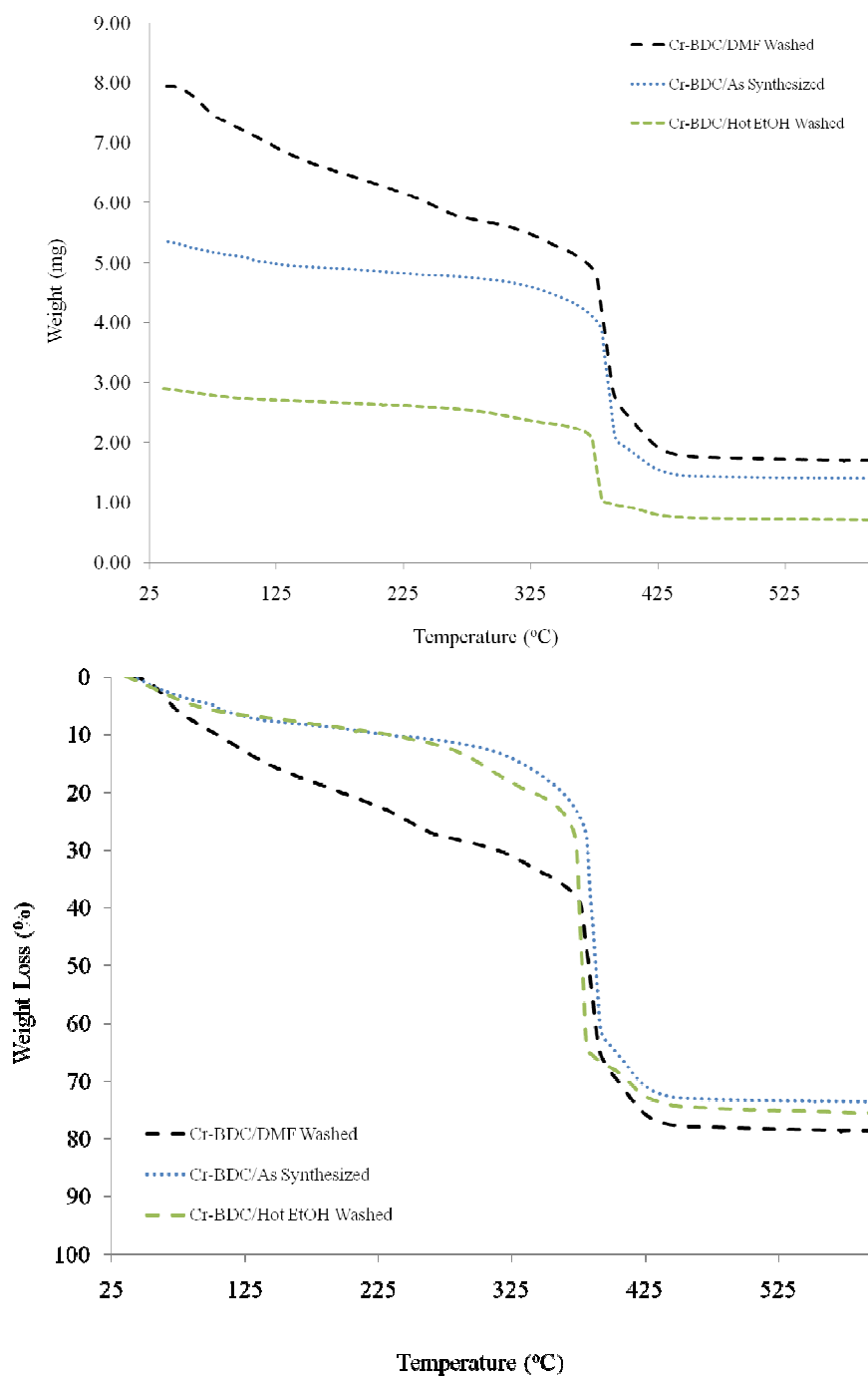


Figure 4.5: TGA pattern of Cr-BDC samples, top (absolute weight loss) & Bottom (% weight loss)

If we shift our attention to percentage weight loss graph, we can see three distinct weight loss zones. Regime I, i.e. from 25 to 150°C accounts for removal of moisture and other volatile materials from the adsorbent surface. For as-synthesized batch and hot ethanol washed batch, the TGA plots overlap in this regime. The reason could be low boiling point for ethanol and readily gets out of the adsorbent pores at higher temperature. Conversely, we could see a continuous sharper degradation for DMF washed sample in the same regime. This is understandable since the boiling point of DMF is 150°C and hence it slowly comes out of the adsorbent surface. Regime II, i.e. from 150°C to 350°C, the rate of weight loss is much slower and approaches towards stability. For most gas adsorption study, this range can be taken to be as ‘stable zone’. Regime III, i.e. beyond 350°C, the Cr-BDC structure collapses. This is perhaps due to the elimination of OH/F groups from the framework. Although the degradation pattern of Cr-BDC samples synthesized in our lab is typical but we can see there is a slight shift in the final degradation temperature. The increasing order in the degradation temperature is $[\text{Cr-BDC}]_{\text{EtOH washed}} < [\text{Cr-BDC}]_{\text{DMF washed}} < [\text{Cr-BDC}]_{\text{as synthesized}}$. This trend can be as a result of removal of solvated impurities. The presence of impurities in one hand increases the degradation temperature but eventually it will result into decrease in effective surface area for gas adsorption. The bulk packing density, which is a function of impurities present are also calculated.

$$\text{Cr-BDC [As synthesized]} = 0.734 \text{ gm/cc}$$

$$\text{Cr-BDC [DMF washed]} = 0.434 \text{ gm/cc}$$

$$\text{Cr-BDC [EtOH washed]} = 0.217 \text{ gm/cc}$$

Thus we can see the packing density data corroborate well with the TGA data.

4.6 Surface Morphology of Cu-BTC

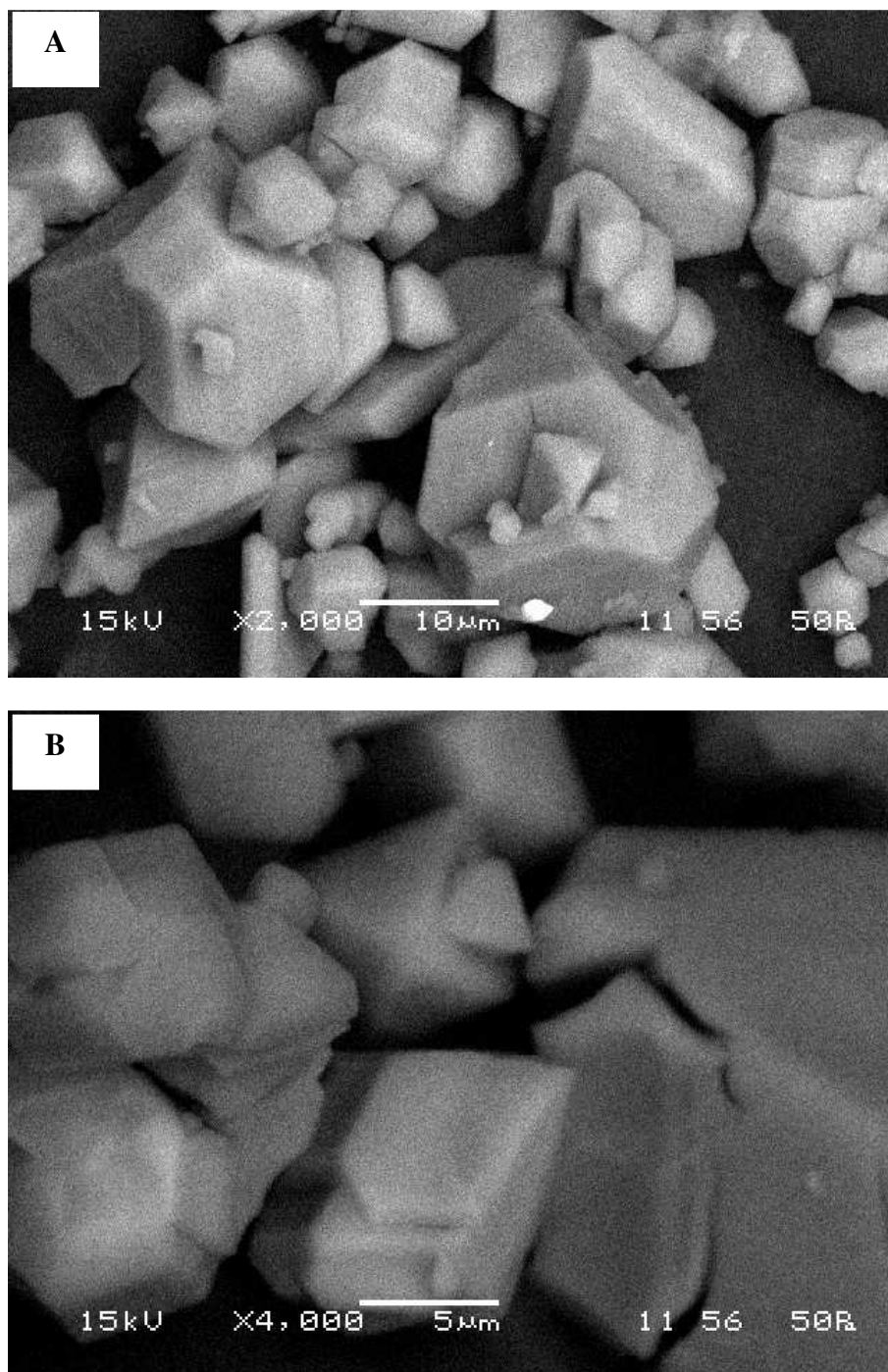
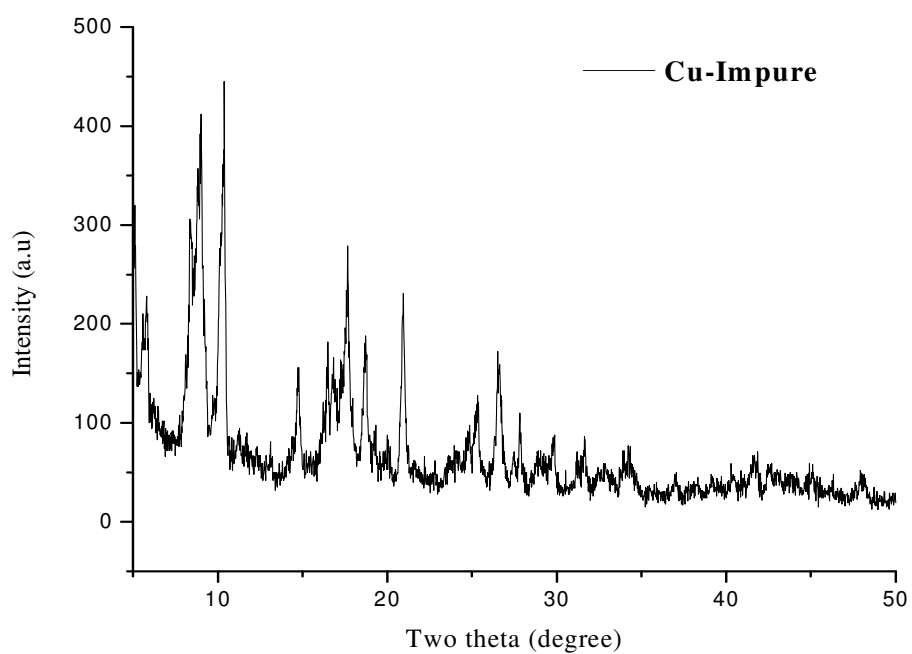


Figure 4.6: SEM images of Cu-BTC samples

From the SEM images, we can rightly conclude the crystals are octahedral in nature with some of them are bigger than the rest. We can also see the agglomeration of some of the smaller crystals. This can possibly be attributed to the improper crystallization of the products. It is also noteworthy to mention that the average size of the Cu-BTC crystals is much bigger than the Cr-BDC crystals.

4.7 The Powder XRD Pattern of Cu-BTC



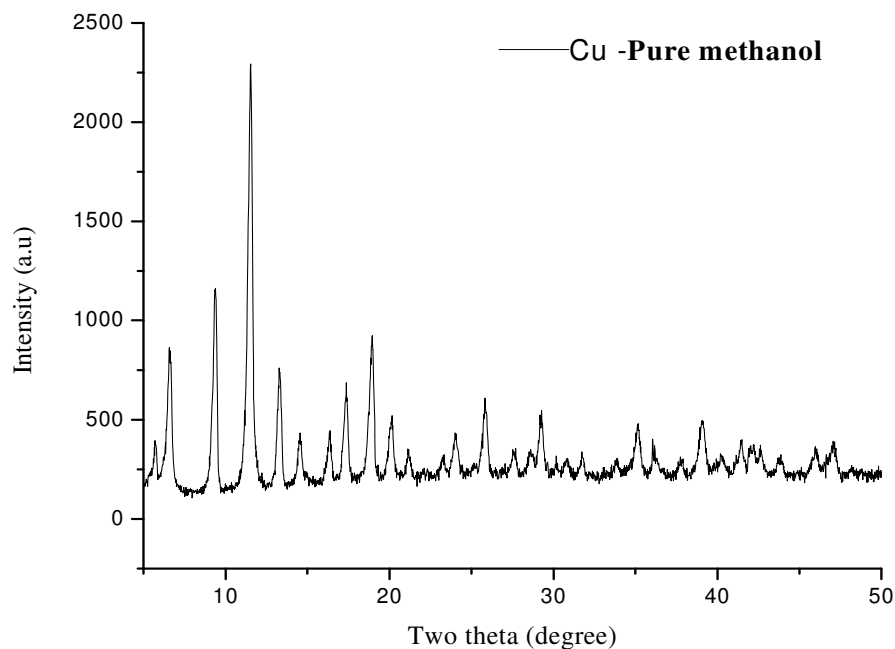


Figure 4.7: Powder XRD pattern of various batches Cu-BTC samples

The XRD pattern corroborates well with published literature data. It is however significant to highlight the striking difference between the XRD profiles of two Cu-BTC samples. Methanol washed sample shows a better refinement in XRD peaks as compared to the original sample. However, Cu-BTC samples show good crystallinity.

4.8 Thermogravimetry Analysis of Cu-BTC Samples

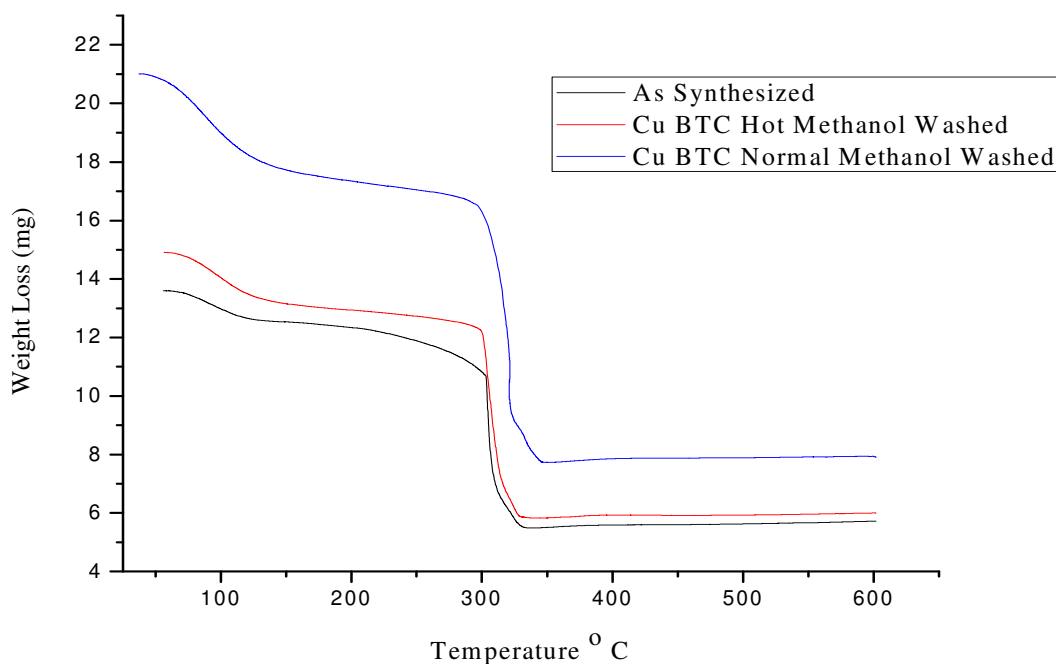


Figure 4.8: TGA pattern of Cu-BDC samples

This typical TGA profile shows three distinct weight loss steps and is similar to TGA profile of Cr BDC. The washed sample shows lesser stability than the as synthesized batch which is attributed to subsequent removal of impurities present, authenticated by the SEM images and XRD patterns. In the range of 25-125°C the weight loss is purely due to removal of moisture and trapped methanol. The second step from 125°C to 275°C is a horizontal plateau, where the weight remains fairly constant. Beyond 275°C the structure collapses.

4.9 Surface Morphology of Zn-BDC

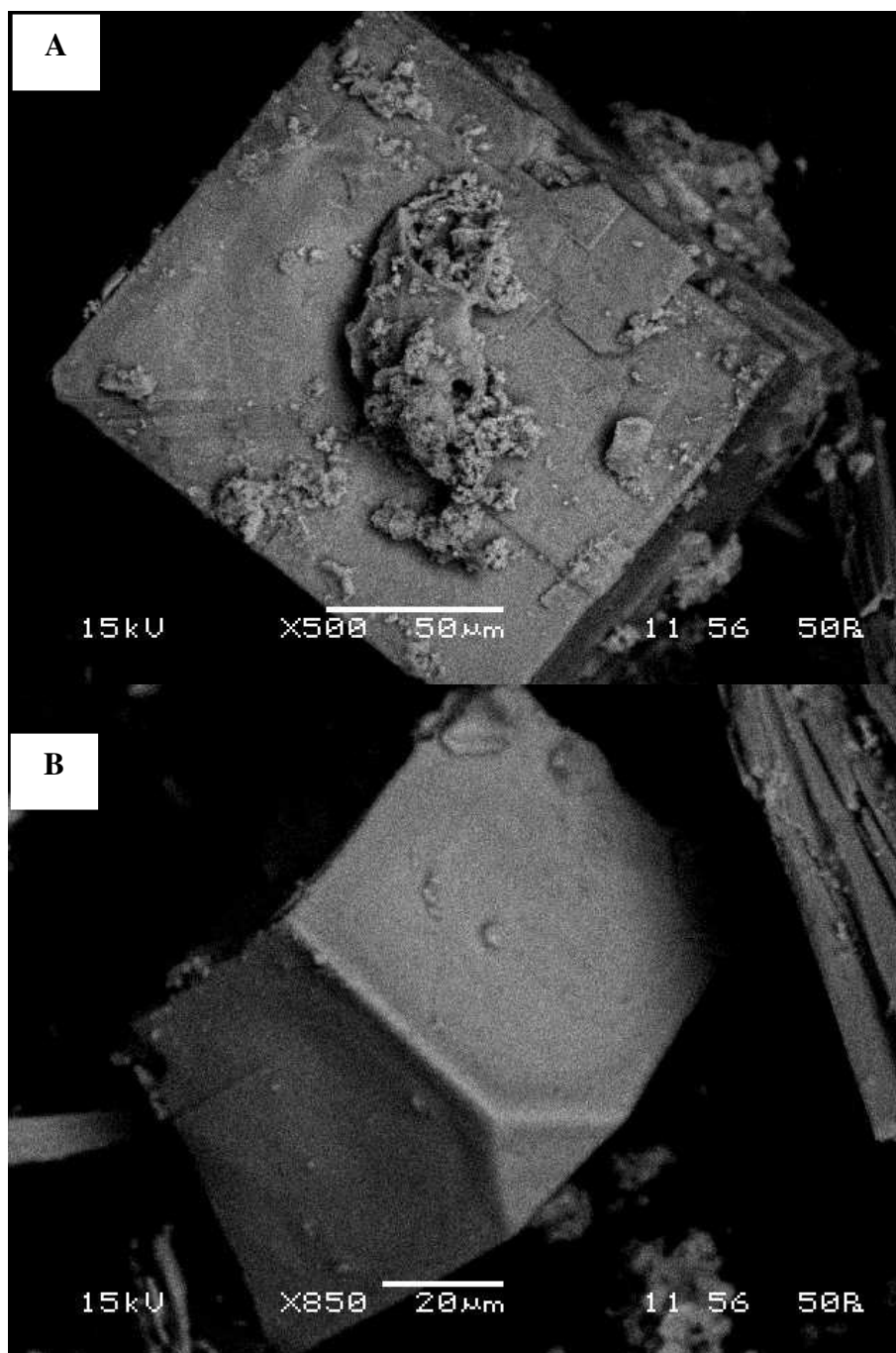
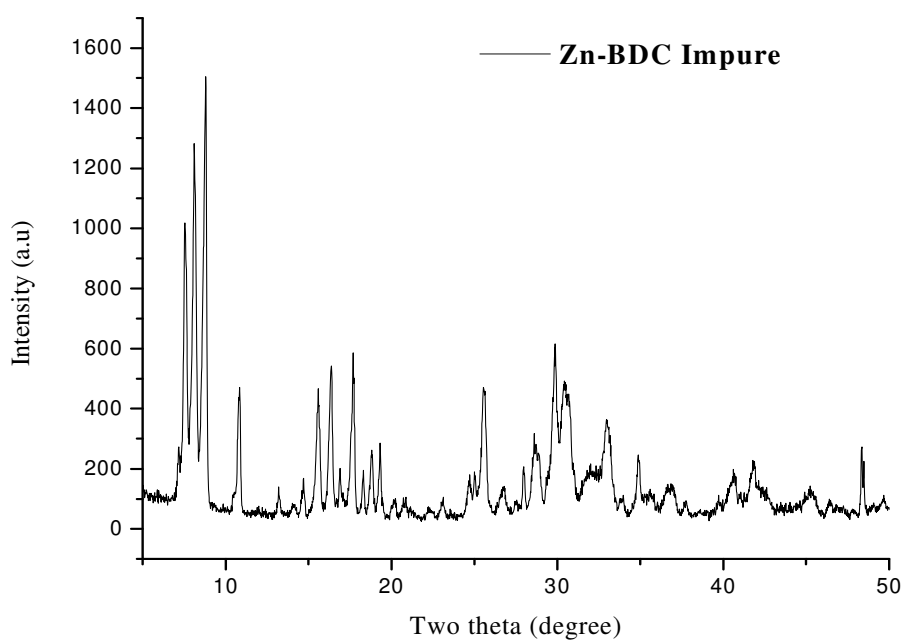


Figure 4.9: SEM images of Cu-BTC samples

The SEM images of both pure and impure batches of Zn-BDC samples are shown. It is however important to notice that unlike Cu-BTC and Cr-BDC samples, Zn-BDC is cubic in nature and the crystal sizes are the biggest amongst all three.

4.10 The Powder XRD Pattern of Zn-BDC



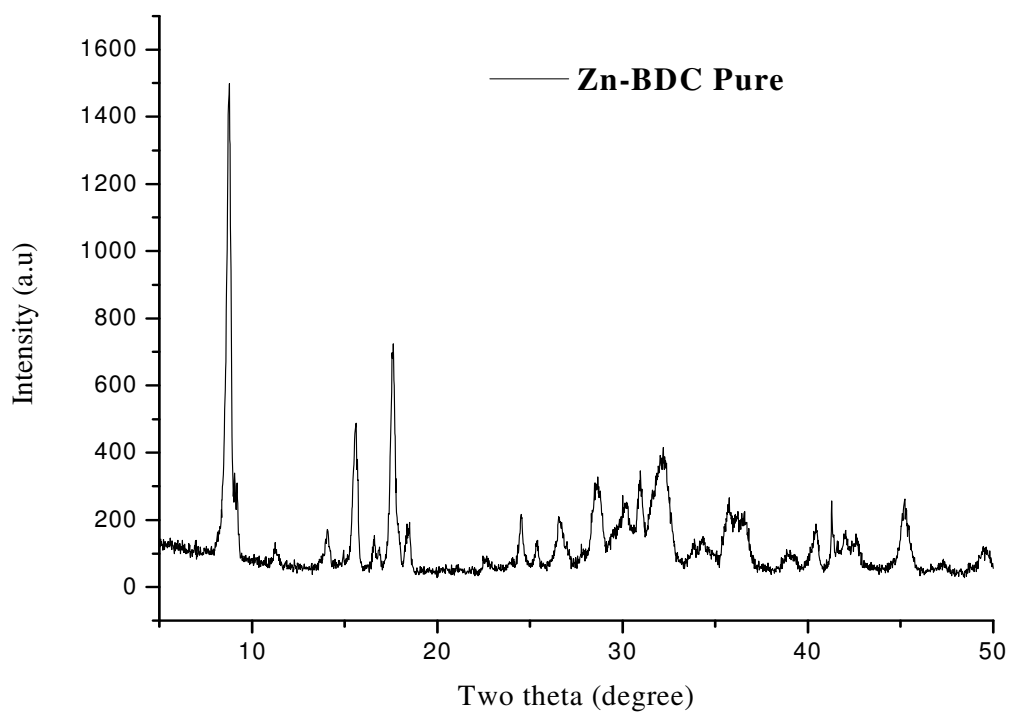


Figure 4.10: Powder XRD pattern of various batches Zn-BDC samples

Just like Cu-BTC and Cr-BDC samples, Zn-BDC too is crystalline in nature. A better post-synthesis treatment reduces the percentage of innate impurities in the sample, leading to good refinement in XRD peaks.

4.11 Thermogravimetry Analysis of Zn-BDC Samples

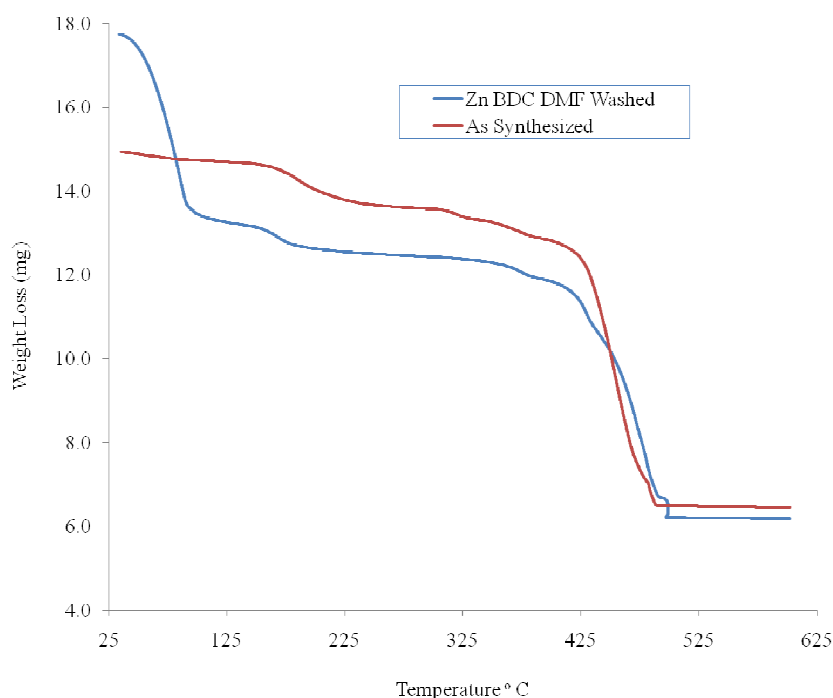


Figure 4.11: TGA pattern of Zn-BDC samples

The absolute weight loss steps for Zn-BDC are shown in the figure. For as-synthesized sample the pattern in weight loss is erratic, although we can conclude that up to 150°C, the minor change in weight loss is due to removal of guest water molecules. From 150°C-400°C the weight loss remained largely stable. Beyond 400°C the structure collapses.

The DMF washed sample too follow a common trail. The initial weight loss is largely due to removal of DMF. The minor shift in degradation profile towards left signifies the removal of impurities due to proper DMF treatment. The packing density data too corroborates this fact, Zn-BDC (as synthesized) = 0.6 gm/cc whereas, Zn-BDC (DMF washed) = 0.483 gm/cc.

CHAPTER 5

CONCLUSIONS & FUTURE SCOPE

Synthesis and characterization of Cu-BTC, Cr-BDC and Zn-BDC samples were successfully carried out in our present study. SEM images confirmed the authenticity of each of the MOFs. Cr-BDC and Cu-BTC were found octahedral in shape whereas Zn-BDC crystals appeared to be cubic in nature. The presence of impurities was not uncommon in MOF synthesis and here as well we had seen reactions leading to the formation of impure by-products. Post synthesis treatments in different organic environments were particularly important in removal of these impurities. Powder XRD patterns validated the crystalline nature of the products formed and thereby degree of purity in various batches owing to different solvent treatments. TGA patterns were typical of specific MOFs synthesized. However, a shift towards low thermal stability had been observed for cases where solvents eliminated impurities. Although it appeared that elimination of impurities decreased the thermal stability of the products but if not, eventually it would lead to reducing the effective surface area which is most crucial in any gas adsorption study. The packing density data nicely corroborated the TGA analysis.

There is a plenty of scope of this present work. It is of paramount importance to actually find the surface area, pore volume and pore size distribution of all the synthesized products. Additionally, newer mechanisms are required to be invented to improve the thermal and chemical stability of synthesized materials.

The same study can be extended in fabricating MOF based membrane. Metal Organic Framework (MOF) based membrane fabrication is relatively a neo-idea that is gaining considerable attention in research community. The whole idea is to impart pertinent properties of specific MOF concerned onto the membrane surface for tuning its morphology meeting specific applications. However, a major bottleneck before success of any such initiation would be synthesizing MOFs in pure form, devoid of any innate or external impurities and having good thermal and chemical stability.

The concept of tuning the pores of a membrane using ‘surface modification technique’ is also gaining momentum and our present study can very well lead to improvising the surface properties of membrane which would on the other hand be useful in ‘nano-filtration’ operations.

REFERENCES

- [1] Yang, R. T., *Gas Separation by Adsorption Processes*, Imperial College Press, London (1997), Chapter-1.
- [2] Ruthven, D. M. and Sun, M. S., *Principle of Adsorption and Adsorption Processes*, Wiley-Interscience, New York, (1984), Chapter-1.
- [3] Guisnet, M. and Gilson, J. P., *Zeolites for Cleaner Technologies*, Imperial College Press, London, (2002), p. 1-2.
- [4] Szostak, R., *Molecular Sieves Principles of Synthesis and Identification*, Blackie Academic & Professional, London, (1998), p. 3.
- [5] Yaghi, O. M., O’Keeffe, M., Ockwig, N. W., Chae, H. K., Eddaoudi, M., and Kim, J., “Reticular Synthesis and the design of New Materials,” *Nature*, **423**, 705-714 (2003).
- [6] Rowsell, J. L. C., and Yaghi, O. M., “Metal–organic frameworks: a new class of porous materials,” *Micropor. Mesopor. Mater.*, **73**, 3-14 (2004).
- [7] Galet, A., Niel, V., Muñoz, M. C., and Real, J. A., “Synergy between Spin Crossover and Metallophilicity in Triple Interpenetrated 3D Nets with the NbO Structure Type,” *J. Am. Chem. Soc.*, **125**, 14224-14225 (2003).
- [8] Ma, B. Q., Sun, H. L., and Gao, S., “The Design and Synthesis of a non-centric Diamond-like Network Based NH_4^+ Ion,” *Chem. Commun.*, 2164-2165 (2003).
- [9] Lo, S. M- F., Chui, S. S- Y., Shek, L. Y., Lin, Z., Zhang, X. X., Wen, G., and Williams, I.D., “Solvothermal Synthesis of a Stable Coordination Polymer with Copper-I-Copper-II Dimer Units: $[\text{Cu}_4\{1,4\text{-C}_6\text{H}_4(\text{COO})_2\}_3(4,4'\text{-bipy})_2]_n$,” *J. Am. Chem. Soc.*, **122**, 6293-6294 (2000).
- [10] Luo, J., Hong, M., Wang, R., Cao, R., Han, L., Yuan, D., Lin, Z., and Zhou, Y., “A Novel Bilayer Cobalt(II)-Organic Framework with Nanoscale Channels Accommodating Large Organic Molecules,” *Inorg. Chem.*, **42**, 4486-4488 (2003).

- [11] Barthelet, K., Marrot, J., Riou, D., and Férey, G., "A Breathing Hybrid Organic-Inorganic Solid with Very Large Pores and High Magnetic Characteristics," *Angew. Chem. Int. Ed.*, **41**, 281-284 (2002).
- [12] Bu, X. H., Tong, M. L., Chang, H. C., Kitagawa, S., and Batten, S. R., "A Neutral 3D Copper Coordination Polymer Showing 1D Open Channels and the First Interpenetrating NbO-Type Network," *Angew. Chem. Int. Ed.*, **43**, 192-195 (2004).
- [13] Hong, J., "[Zn₂(BTDA)(bpy)(H₂O)].0.5bpy: a new three-dimensional metal-organic framework constructed from flexible and rigid mixed ligands," *J. Mol. Struct.*, **752**, 166-169 (2005).
- [14] Dunbar, K. R., and Heintz, R. A., "Chemistry of Transition Metal Cyanide Compounds: Modern Perspectives," *Prog. Inorg. Chem.*, **45**, 283-391 (1997).
- [15] Gramaccioli, C. M., "The crystal structure of zinc glutamate dehydrate," *Acta Cryst.*, **21**, 600-605 (1966).
- [16] Okada, K., Kay, M.I., Cromer, D.T., and Almodovar, I., "Crystal Structure by Neutron Diffraction and the Antiferroelectric phase Transition in Copper Formate Tetrahydrate," *J. Chem. Phys.*, **44**, 1648-1653 (1966).
- [17] Jarvis, J. A. J., "The crystal structure of a complex of cupric chloride and 1:2:4-triazole," *Acta Cryst.*, **15**, 964-966 (1962).
- [18] Sterling, C., "Crystal Structure of Weddellite," *Science*, **146**, 518-519 (1964).
- [19] Robl, C., "Water Clustering in the Zeolite-like Channel Structure of Na₂Zn[C₆H₂(COO)₄].9H₂O," *Mater. Res. Bull.*, **27**, 99-107 (1992).
- [20] Davis, M. E., "Ordered Porous Materials for Emerging Applications," *Nature*, **417**, 813-821 (2002).
- [21] Mueller, U., Schubert, M., Teich, F., Puetter, H., Schierle-Arndt, K., and Pastré, J., "Metal-organic Frameworks-Prospective Industrial Applications," *J. Mater. Chem.*, **16**, 626-636 (2006).

- [22] Li, H., Eddaoudi, M., O’Keeffe, M., and Yaghi, O. M., “Design and Synthesis of an Exceptionally Stable and Highly Porous Metal-organic Framework,” *Nature*, **402**, 276-279 (1999).
- [23] Sarkisov, L., Düren, T., and Snurr, R.Q., "Molecular modeling of adsorption in novel nanoporous metal-organic materials," *Mol. Phys.*, **102**, 211-221 (2004)
- [24] Skoulidas, A. I., and Sholl, D. S., “Self-diffusion and transport diffusion of light gases in metal-organic framework materials assessed using molecular dynamics simulation,” *J. Phys. Chem. B*, **109**, 15760-15768 (2005).
- [25] Düren, T., and Snurr, R.Q., “Assessment of Isorecticular Metal-Organic Frameworks for Adsorption Separations: A Molecular Simulation Study of Methane/*n*-Butane Mixtures,” *J. Phys. Chem. B*, **108**, 15703-15708 (2004).
- [26] Kawakami, T., Takamizawa, S., Kitagawa, Y., Maruta, T., Mori, W., and Yamaguchi, K., “Theoretical studies of spin arrangement of adsorbed organic radicals in metal-organic nanoporous cavity,” *Polyhedron*, **20**, 1197-1206 (2001).
- [27] Eddaoudi, M., Li, H., and Yaghi, O. M., “ Highly Porous and Stable Metal-Organic Frameworks: Structure, Design and Sorption Properties,” *J. Am. Chem. Soc.*, **122**, 1391-1397 (2000).
- [28] Eddaoudi, M., Kim, J., Rosi, N., Vodak, D., Wachter, J., O’Keeffe, M., Yaghi, O. M., “Systematic Design of Pore Size and Functionality in Isorecticular MOFs and Their Application in Methane Storage,” *Science*, **295**, 469-472 (2002).
- [29] Bourrelly, S., Llewellyn, P. L., Serre, C., Millange, F., Loiseau, T., and Férey, G., “Different Adsorption Behaviors of Methane and Carbon Dioxide in the Isotypic Nanoporous Metal Terephthalates MIL-53 and MIL-47,” *J. Am. Chem. Soc.*, **127**, 13519-13521 (2005).

- [30] Millward, A. R., and Yaghi, O. M., “Metal-Organic Frameworks with Exceptionally High Capacity for Storage of Carbon Dioxide at Room Temperature,” *J. Am. Chem. Soc.*, **127**, 17998-17999 (2005).
- [31] Senkovska, I. and Kaskel, S., “High pressure methane adsorption in the metal-organic frameworks $\text{Cu}_3(\text{btc})_2$, $\text{Zn}_2(\text{bdc})_2\text{dabco}$, and $\text{Cr}_3\text{F}(\text{H}_2\text{O})_2\text{O}(\text{bdc})_3$,” *Micropor. Mesopor. Mater.*, **112**, 108-115 (2008).
- [32] Llewellyn, P.L., Bourrelly, S., Serre, C., Vimont, A., Daturi, M., Hamon, L., Weireld, G. D., Chang, J. -S., Hong, D. -Y., Hwang, Y. K., Jhung, S. H., Férey, G., “High Uptakes of CO_2 and CH_4 in Mesoporous Metal-Organic Frameworks MIL-100 and MIL-101,” *Langmuir*, **24**, 7245-7250 (2008).
- [33] Llabres i Xamena, F. X., Abad, A., Corma, A., and Garcia, H., “MOFs as catalysts: Activity, reusability and shape-selectivity of a Pd-containing MOF,” *J. Catal.*, **250**, 294-298 (2007).
- [34] Schlichte, K., Kratzke, T., and Kaskel, S., “Improved synthesis, thermal stability and catalytic properties of the metal-organic framework compound $\text{Cu}_3(\text{BTC})_2$,” *Micropor. Mesopor. Mater.*, **73**, 81-88 (2004).
- [35] Gomez-Lor, B., Gutierrez-Puebla, E., Iglesias, M., Monge, M. A., Ruiz-Valero, C., and Snejko, N., “Novel 2D and 3D Indium Metal-Organic Frameworks: Topology and Catalytic Properties,” *Chem. Mater.*, **17**, 2568-2573 (2005).
- [36] Yamada, Y. M. A., Maeda, Y., and Uozumi, Y., “Novel 3D Coordination Palladium-Network Complex: A Recyclable Catalyst for Suzuki-Miyaura Reaction,” *Org. Lett.*, **8**, 4259-4262 (2006).
- [37] Janiak, C., “Engineering coordination polymers towards applications,” *Dalton Trans.*, 2781-2804 (2003).
- [38] Hagrman, P. J., Hagrman, D., and Zubieta, J., “Organic-Inorganic Hybrid Materials: From Simple Coordination Polymers to Organodiamine-Templated Molybdenum Oxides, ” *Angew. Chem. Int. Ed.*, **38**, 2638-2684 (1999).

- [39] Blake, A. J., Champness, N. R., Hubberstey, P., Li, W. S., Withersby, M. A., and Schröder, M., “Inorganic crystal engineering using self-assembly of tailored building-blocks,” *Coordination Chem. Rev.*, **183**, 117-138 (1999).
- [40] Moulton, B., and Zaworotko, M. J., “From Molecules to Crystal Engineering: Supramolecular Isomerism and Polymorphism in Network Solids,” *Chem. Rev.*, **101**, 1629-1658 (2001).
- [41] Rao, C. N. R., Natarajan, S., and Vaidhyanathan, R., “Metal Carboxylates with Open Architectures,” *Angew. Chem. Int. Ed.*, **43**, 1466-1496 (2004).
- [42] Xiao, B., Wheatley, P. S., Zhao, X., Fletcher, A. J., Fox, S., Rossi, A. G., Megson, I. L., Bordiga, S., Regli, L., Mark Thomas, K., and Morris, R. E., “High-Capacity Hydrogen and Nitric Oxide Adsorption and Storage in a Metal-Organic Framework,” *J. Am. Chem. Soc.*, **129**, 1203-1209 (2007).
- [44] Chui, S. S.-Y., Lo, S. M.-F., Charmant, J. P. H., Orpen, A. G., and Williams, I. D., “A Chemically Functionalizable Nanoporous material $[\text{Cu}_3(\text{TMA})_2(\text{H}_2\text{O})_3]_n$,” *Science*, **283**, 1148-1150 (1999).
- [45] Krungleviciute, V., Lask, K., Heroux, L., Migone, A. D., Lee, J. -Y., Li, J., and Skoulidas, A., “Argon Adsorption on $\text{Cu}_3(\text{Benzene-1,3,5-tricarboxylate})_2(\text{H}_2\text{O})_3$ Metal-Organic Framework,” *Langmuir*, **23**, 3106-3109 (2007).
- [46] Férey, G., Mellot-Draznieks, C., Serre, C., Millange, F., Dutour, J., Surblé S., and Margiolaki, I., “A Chromium Terephthalate-Based Solid with Unusually Large Pore Volumes and Surface Area,” *Science*, **309**, 2040-2042 (2005).
- [47] Lebedev, O. I., Millange, F., Serre, C., Van Tendeloo, G., and Férey, G., “First Direct Imaging of Giant Pores of the Metal-Organic Framework MIL-101,” *Chem. Mater.*, **17**, 6525-6527 (2005).
- [48] Jinchun Liu, Jeffrey T. Culp, Sittichai Natesakhawat, Bradley C. Bockrath, Brian Zande, S. G. Sankar, Giovanni Garberoglio, and J. Karl Johnson, “Experimental and Theoretical Studies of Gas Adsorption in $\text{Cu}_3(\text{BTC})_2$ ” *J. Phys. Chem. C.*, **111**, 9305-9313 (2007).

- [49] Wang, Q.M., Shen, D., Bülow, M., Lau, M. L., Deng, S., Fitch, F. R., Lemcoff, N. O., Semanscin, J., “Metallo-organic molecular sieve for gas separation and purification,” *Micropor. Mesopor. Mater.*, **55**, 217-230 (2002).
- [50] Vishnyakov, A., Ravikovitch, P. I., Neimark, A. V., Bülow, M., Wang, Q. M., “Nanopore structure and sorption properties of Cu-BTC metal-organic framework,” *Nano Lett.*, **3**, 713-718 (2003).
- [51] Mueller, U., Schubert, M., Teich, F., Puetter, H., Schierle-Arndt, K., and Pastré, J., “Metal-organic Frameworks-Prospective Industrial Applications,” *J. Mater. Chem.*, **16**, 626-636 (2006).
- [52] Millward, A. R., and Yaghi, O. M., “Metal-Organic Frameworks with Exceptionally High Capacity for Storage of Carbon Dioxide at Room Temperature,” *J. Am. Chem. Soc.*, **127**, 17998-17999 (2005).
- [53] Rowsell, J. L. C., and Yaghi, O. M., “Effects of Functionalization, Catenation, and Variation of the Metal Oxide and Organic Linking Units on the Low-Pressure Hydrogen Adsorption Properties of Metal-Organic Frameworks,” *J. Am. Chem. Soc.*, **128**, 1304-1315 (2006).
- [54] Krungleviciute, V., Lask, K., Heroux, L., Migone, A. D., Lee, J. -Y., Li, J., and Skoulidas, A., “Argon Adsorption on $\text{Cu}_3(\text{Benzene-1,3,5-tricarboxylate})_2(\text{H}_2\text{O})_3$ Metal-Organic Framework,” *Langmuir*, **23**, 3106-3109 (2007).
- [55] Jiangfeng Yang, Qiang Zhao, Jinping Li, and Jinxiang Dong, “Synthesis of metal-organic framework MIL-101 in TMAOH- $\text{Cr}(\text{NO}_3)_3$ - H_2BDC - H_2O and its hydrogen-storage behavior,” *Microporous and Mesoporous Materials*, **130**, 174–179 (2010).
- [56] Do-Young Hong, Young Kyu Hwang, Christian Serre, Ge´rard Fe´rey, and Jong-San Chang, “Porous Chromium Terephthalate MIL-101 with Coordinatively Unsaturated Sites: Surface Functionalization, Encapsulation, Sorption and Catalysis,” *Adv. Funct. Mater.*, **19**, 1537–1552 (2009).

- [57] Li, Y., and Yang, R.T., “Hydrogen Storage in Metal-Organic and Covalent-Organic Frameworks by Spillover,” *AIChE J.*, **54**, 269-279 (2008).
- [58] Li, H., Eddaoudi, M., O’Keeffe, M., and Yaghi O.M., “Design and synthesis of an exceptionally stable and highly porous metal–organic framework,” *Nature*, **402**, 276–279 (1999).
- [59] Huang, L., Wang, H., Chen, J., Wang, Z., Sun, J., and Zhao, D., “Synthesis, morphology control, and properties of porous metal–organic coordination polymers,” *Micropor Mesopor Mater*, **58(2)**, 105–114 (2003).
- [60] Rowsell, J. L. C., Milward, A. R., Park, K. S., and Yaghi, O. M., “Hydrogen sorption in functionalized metal–organic frameworks,” *J. Am. Chem. Soc.* 126(18), 5666–7 (2004).
- [61] Panella, B., and Hirscher, M., “Hydrogen physisorption in metal– organic porous crystals,” *Adv. Mater.* **17(5)**, 538–41 (2005).
- [62] Panella, B., Hirscher, M., Putter, H., and Muller, U., “Hydrogen adsorption in metal–organic frameworks: Cu-MOFs and Zn-MOFs compared,” *Adv Funct Mater*, 16(4), 520–4 (2006).
- [63] Henrik Fanø, Clausen., Rasmus Damgaard, Poulsen., Andrew, D. Bond., Marie-Agnes, S. Chevallier., Bo and Brummerstedt, Iversen., “Solvothermal synthesis of new metal organic framework structures in the zinc–terephthalic acid–dimethyl formamide system,” *Solid State Chemistry*, **178**, 3342–3351(2005).
- [64] Jinping, Li., Shaojuan, Cheng., Qiang, Zhao., Peipei, Long., and Jinxiang, Dong., “Synthesis and hydrogen-storage behavior of metal–organic framework MOF-5,” *Int. J. of Hydrogen Energy*, **34**, 1377-1382 (2009).

RESEARCH PUBLICATIONS

Conference Proceedings

[I] Gaurav Chandrakar, and Pradip Chowdhury, “Microporous Metal Organic Frameworks as a Potential Medium for CO₂ Capture,” **3rd International Congress of Environmental Research, September 16-18, University of Mauritius, Reduit, Mauritius.**

(II) Pradip Chowdhury, Shankarnarayanan Hariharan, and Gaurav Chandrakar, “Fabrication of Metal Organic Framework (MOF) based Membrane,” **Submitted to AIChE Annual Conference 2011, Minneapolis, USA.**